University of Massachusetts Amherst
ScholarWorks@UMass Amherst

Open Access Dissertations

9-2012

Molecular mechanisms regulating Complement Receptor 3-mediated phagocytosis of Borrelia burgdorferi

Kelly Lynn Hawley
University of Massachusetts Amherst, khawley@vasci.umass.edu

Follow this and additional works at: https://scholarworks.umass.edu/open_access_dissertations

Part of the Biotechnology Commons

Recommended Citation
Hawley, Kelly Lynn, "Molecular mechanisms regulating Complement Receptor 3-mediated phagocytosis of Borrelia burgdorferi" (2012). *Open Access Dissertations*. 645.
https://doi.org/10.7275/sa1d-j556 https://scholarworks.umass.edu/open_access_dissertations/645

This Open Access Dissertation is brought to you for free and open access by ScholarWorks@UMass Amherst. It has been accepted for inclusion in Open Access Dissertations by an authorized administrator of ScholarWorks@UMass Amherst. For more information, please contact scholarworks@library.umass.edu.

MOLECULAR MECHANISMS REGULATING COMPLEMENT RECEPTOR 3-MEDIATED PHAGOCYTOSIS OF *BORRELIA BURGDORFERI*

A Dissertation Presented

by

KELLY L. HAWLEY

Submitted to the Graduate School of the

University of Massachusetts Amherst in partial fulfillment

of the requirements for the degree of

DOCTOR OF PHILOSOPHY

September 2012

Department of Animal Biotechnology and Biomedical Sciences

© Copyright by Kelly L. Hawley 2012

All rights Reserved

MOLECULAR MECHANISMS REGULATING COMPLEMENT RECEPTOR 3-MEDIATED PHAGOCYTOSIS OF *BORRELIA BURGDORFERI*

A Dissertation Presented

by

KELLY L. HAWLEY

Approved as to style and content by:

_____
Juan Anguita, Chair

_____
Barbara A. Osborne, Member

_____
Lisa M. Minter, Member

_____
Justin D. Radolf, Member

_____
Rafael A. Fissore, Department Head
Department of Veterinary & Animal Sciences

DEDICATED TO

This dissertation is dedicated to my husband, Aaren Hawley for all of his love, encouragement and understanding throughout the process of this degree because without his support, this work would not have been possible. In addition, I would like to dedicate this work to my daughter, Kailyn Hawley and my son, Logan Hawley as a symbol that nothing is out of reach and encouragement for them to aim for the stars.

ACKNOWLEDGEMENTS

I would like to express my greatest appreciation to my mentor, Dr. Juan Anguita for making me part of his lab family and helping me grow as a scientist. He always pushed me to achieve more than I thought I was capable of achieving. I appreciate the efforts of Dr. Barbara Osborne, Dr. Lisa Minter and Dr. Justin Radolf as members of my dissertation committee and for their endless support and guidance. To Dr. Justin Radolf, Dr. Mercedes Rincon, Dr. Melissa Caimano, Dr. Juan Salazar, Dr. Robin Ingalls, Tonya Bates, Dr. Chris Olson, Dr. Nicolas Navasa and Dr. Juan Manuel Iglesias for their help and contribution to my work.

I would like to thank my friends and coworkers for their support during the last four years. This gratitude goes to Tonya Bates, Dr. Chris Olson, Dr. Hooman Izadi, Dr. Nicolas Navasa, Dr. Juan Manuel Iglesias, Dr. Abhigyan Som, Furkan Ayaz, Tina Arieta and the entire "Osguiter" quadrant.

Finally, I would like to thank my family for supporting my dream of being a "Professional Student" because all of their encouragement allowed me to be successful.

ABSTRACT

MOLECULAR MECHANISMS REGULATING COMPLEMENT RECEPTOR 3-MEDIATED PHAGOCYTOSIS OF *BORRELIA BURGDORFERI*

SEPTEMBER 2012

KELLY L. HAWLEY

B.S., UNIVERSITY OF MASSACHUSETTS, AMHERST

Ph.D., UNIVERSITY OF MASSACHUSETTS, AMHERST

Directed by: Professor Juan Anguita

The macrophage receptors that mediate phagocytosis of *Borrelia burgdorferi*, the Lyme disease spirochete, are unknown despite this cell type's importance in promoting pathogen clearance and inflammation-mediated tissue damage. We now demonstrate that the β2 integrin, Complement Receptor 3 (CR3), mediates the phagocytosis of opsonized and non-opsonized spirochetes by murine macrophages and human monocytes. Although, expression of the surface proteins, CspA and OspE, protects *B. burgdorferi* from complement-mediated phagocytosis, the versatility of CR3 counteracts the ability of *B. burgdorferi* to interfere with complement activation and complement-derived opsonins, thus minimizing the bacteria's anti-complement strategy. Interaction of the spirochete with the integrin is not sufficient to internalize *B. burgdorferi*; however, phagocytosis occurs when the GPI-anchored protein, CD14, is coexpressed in CHO-CR3 cells. CR3-mediated phagocytosis occurs independently of MyD88-induced or inside-out signals but requires the

translocation of the integrin to cholesterol rich membrane microdomains. Interestingly, the absence of CR3 leads to marked increases in production of TNF *in vitro* and *in vivo*, in spite of reduced spirochetal uptake. Overall, our data establish CR3 as a MyD88-independent phagocytic receptor for *B. burgdorferi* that also participates in the modulation of the proinflammatory output of macrophages.

Macrophages are critical cellular components of the immune response to infectious agents. During infection with *B. burgdorferi*, macrophages infiltrate the cardiac tissue and induce the activation of invariant NKT cells, leading to the production of the protective cytokine IFNγ. The interaction of macrophages with infectious agents leads to the activation of several signaling cascades, including mitogen activated protein kinases, such as p38 MAP kinase. We now demonstrate that p38 MAP kinase-mediated responses are critical components to the immune response during infection with *B. burgdorferi*. The inhibition of p38 MAP kinase does not alter the ability of macrophages to phagocytose *B. burgdorferi*; however, inhibition of p38 during infection with *B. burgdorferi* results in increased carditis. Through the generation of transgenic mice that express a dominant negative form of p38 MAP kinase specifically in macrophages, we demonstrate that this kinase regulates the production of the iNKT attracting chemokine, MCP-1 and the infiltration of these cells to the cardiac tissue during infection. Overall, the inhibition of p38 MAP kinase during infection with *B. burgdorferi* specifically in macrophages results in the deficient infiltration of iNKT cells and their diminished production of IFNγ, leading to increased bacterial burdens and inflammation. These results show that p38 MAP kinase provides critical checkpoints for the protective immune response to the spirochete during infection of the heart.

TABLE OF CONTENTS

Page

LIST OF TABLES

LIST OF FIGURES

Figure Page

CHAPTER I

INTRODUCTION

Lyme disease

In the fall of 1976, following an outbreak of juvenile rheumatoid arthritis of unknown origin in Old Lyme, Connecticut, an investigation was led by Yale School of Medicine's Alan Steere and Stephen Malawista; the cluster of arthritis-like conditions became known as Lyme disease. Willy Burgdorfer, Alan Barbour, and Jorge Benach isolated and identified the spirochetal bacterium, *Borrelia burgdorferi,* as the causative agent of Lyme disease in 1982 (1). Three other species of the genus *Borrelia* have since been identified to cause Lyme disease. In the United Sates, *B. burgdorferi sensu stricto* is the sole etiologic agent of Lyme disease. However, *B. afzelii* and *B. garinii* are restricted to Europe and Asia (Table 1.1); these agents of disease are collectively referred to as *B. burgdorferi sensu lato*.

According to the Centers for Disease Control and Prevention, Lyme disease is the most common vector-borne disease in the United States. Lyme disease commonly begins with an annular skin rash known as *erythema migrans* (EM) at the tick bite location in 70-80% of humans within approximately 7 days of infection with *B. burgdorferi* (Stage I, Lyme disease) (2, 3). Concurrently with the local inflammatory response, individuals may experience fatigue, chills, headache and muscle and joint pain (4). If left untreated, the spirochete disseminates into the bloodstream and invades multiple systems and organs (Stage II) causing a variety of clinical symptoms. The early dissemination stage takes place in the first few days to weeks post tick bite with additional EM lesions on different body areas and other symptoms, such as Bells' palsy, meningitis, heart palpitation and asymmetric swelling

of large joints (3). Lack of treatment may result in the late form of infection (Stage III) with further complications caused by damage to nerves, joints and the cardiac tissue. It is believed that the pathology of the infection is the result of locally activated immune cells and the ensuing inflammatory response.

Enzoonotic life cycle of *B. burgdorferi*

Lyme disease is a zoonotic, vector borne disease where *B. burgdorferi* is transmitted by hard-bodied ticks of the *Ixodes* complex, particularly *Ixodes scapularis* and *I. pacificus* in the United States. In addition to *B. burgdorferi*, *I. scapularis,* more commonly known as the black-legged tick, can act as the vector for other pathogens including *Anaplasma phagocytophilum* and *Babesia microti*. The life cycle of *B. burgdorferi* depends intimately on the two-year life cycle of *I. scapularis* (Fig. 1.1), which consists of three developmental stages: larva, nymph and the adult. The female tick lays her eggs in early spring of the first year, which hatch into the larvae stage during summer. Larvae take the first blood meal by feeding on birds and small rodents, such as the white-footed mouse (*Peromyscus leucopus*) *(5)*, which serve as a reservoir of the infectious agent. Following the first blood meal, ticks molt into nymphs during the early fall and then lay dormant through the winter months. In the late spring to early summer of the second year, nymphs quest for a second blood meal usually on small animals such as rodents, but also dogs and humans. However, humans and dogs are not part of the enzootic life cycle of *B. burgdorferi* and they are considered dead-end hosts. Nymphs mature into adult ticks that feed a final time on large mammals, especially the white tailed deer, but also dogs or humans. The final step of the life cycle can

be completed in the late fall or early spring; following mating, adult female ticks fall off the mammal and lay eggs prior to dying.

The biology of *B. burgdorferi*

B. burgdorferi is 0.2 to 0.3 micrometers wide, 20 to 30 micrometers in length and has periplasmic flagella that extend inward along the cell cylinder beneath an outer membrane sheath giving the spirochete a distinctive flat-wave morphology (Fig. 1.2) (6). The unique rotating flagellum allows the organism to migrate to distant tissues by posteriorly propagating planar waves (7). The outer membrane is essential for organism viability and has been extensively studied because of its importance in vaccine development and the induction of proinflammatory responses in the host. The entire genomes of multiple *B. burgdorferi* strains, including the type strain B31, have been sequenced. The unusual genome includes a linear chromosome approximately one megabase in size with 28.6% G+C content, in addition to numerous linear and circular plasmids (8). *B. burgdorferi* does not encode for any known toxins or secretory systems, so the disease is believed to be mediated by the host's inflammatory immune response to the bacteria. More than 90% of the plasmid-encoded genes are unique to *B. burgdorfer*i, without homologs in any other organisms, suggesting that they encode proteins with functions pertinent to the distinctive lifestyle of the spirochete (8).

B. burgdorferi may persist in the midgut of the tick for an extended period of time with limited nutrients between feedings; however, the bacteria has adapted well to surviving in two different environments. Once the tick is attached to the mammalian host, spirochete surface protein expression is altered as a result of the increased temperature and nutrients, in

addition to a reduction in the pH, thus allowing the spirochetes to be transmitted to the host in a 40 to 48 hour time frame (9, 10). Lipoproteins are distributed throughout the outer leaflet of the inner membrane (cytoplasmic membrane) and both the inner and the outer leaflets of the outer membrane. Outer surface lipoprotein (Osp) A is expressed at high levels on the surface of the spirochete while in the unfed tick midgut and is involved in the attachment of *B. burgdorferi* to this tissue through its interaction with the receptor, TROSPA (11). The down-regulation of OspA during the blood meal allows the spirochete to migrate to the salivary gland from where they are transmitted to the mammalian host (12). This process also requires the upregulation of other genes, including those controlled by RpoS, such as OspC (13-16).

Innate Immune Response to *B. burgdorferi*

The initial detection of a pathogen by the host relies on pathogen recognition receptors (PRRs) and pathogen associated molecular patterns (PAMPs). Toll receptors were first identified in *Drosophila* and later demonstrated to protect flies from fungal infections, bringing to light the importance of the ability of the innate immune system to recognize microorganisms with the aid of surface receptors (17, 18). The mammalian homolog proteins were designated Toll-like receptors (TLRs) (19). The TLR family is evolutionarily conserved from *C. elegans* to mammals and extensively characterized. Functional assays revealed that TLRs were PRR with the ability to detect specific molecules such as microbial lipids, carbohydrates, nucleic acids and proteins among pathogens that are collectively referred to as pathogen-associated molecular patterns (PAMPs). Notably, these PAMPs are not found in mammals thus reducing the possibility of an autoimmune mediated attack but

are essential for initiation of a fast immune response until a more specific response can be developed by the adaptive immune system. This activation aids recruitment of innate immune cells and ultimately clearance of the pathogen.

Individual microbial ligands or synthetic mimics provide valuable delineation of signaling events and biological responses following recognition; however this does not reflect the complexity of an intact microorganism. The identification of Borrelial lipoproteins as PAMPs was a milestone in the understanding of macrophage response to the spirochete (20-25). *B. burgdorferi* is recognized by several TLRs, including TLR1/2 that recognize triacylated proteins present in the spirochete as well as those present exclusively on endosomal compartments, such as TLR8 (26). Notably, the internalization of *B. burgdorferi* greatly enhances the proinflammatory response by macrophages and changes it qualitatively, leading to the production of type I interferons. TLRs recruit adaptor molecules such as myeloid differentiation gene 88 (MyD88) leading to the activation of signaling cascades that result in the production of proinflammatory cytokines (TNF, IL-12, IL-1β and IL-18), chemokines (MCP-1 and KC) and adhesion molecules (ICAM-1, E-selectin) as well as Type I interferons (27-29). Experiments performed with MyD88 deficient mice demonstrated that MyD88 plays a critical role in bacterial clearance and the induction of a full proinflammatory response (30, 31) (32, 33). All of these studies have thus demonstrated that MyD88 exerts a dual action during the interaction of the immune system cells with *B. burgdorferi*.

Mitogen-activated protein (MAP) kinases are activated in response to extracellular stimulation of multiple triggers such as proinflammatory cytokines (e.g. TNF and IL-1β), TLR stimulation in a MyD88-dependent manner, as well as physical-chemical changes in the

extracellular milieu caused by environmental stress then modulating the activation response of the cell (34-39). Several MAP kinase pathways have been described in mammals that are activated by phosphorylation of Thr and Tyr residues by dual-specificity kinases, specifically p38 MAPK is activated by MKK3 and MKK6 (34, 40-46). *B. burgdorferi* is able to induce p38 MAP kinase activity and the kinase can control the proinflammatory response in phagocytic cells by regulating activation of NF-κB in a MSK1-dependent fashion (36, 47). P38 MAP kinase has been shown to regulate actin polymerization during cellular movement (which mimics to a certain extent phagocytosis), in a process that is dependent on Hsp27, a substrate of the kinase and the integrin activation complex component, Paxillin. However, the role of p38 MAP kinase on phagocytosis and control of inflammation during infection with *B. burgdorferi* is currently unknown.

Phagocytosis

Numerous cell types interact with *B. burgdorferi* through PRRs other than TLRs, such as C-type lectins and integrins (48-50). Integrins belong to several β groups and are involved in cell adhesion to a variety of ligands, in addition to cell attachment and migration. The recruitment of phagocytic cells to infected areas is essential for bacterial clearance and the modulation of the cytokine environment (51). However, the interaction of *B. burgdorferi* with macrophages has been predominately focused on the induction of proinflammatory cytokines.

Phagocytosis is defined as the internalization of particles of 1μm or larger and requires the initiation of specific signaling pathways that result in actin polymerization and the internalization of the microorganism. Macrophages are a critical part of the response to

B. burgdorferi, especially for the control of spirochetal numbers in the heart that intimately associate with the production of the macrophage-activating cytokine, IFNγ, which enhances the phagocytic capacity of macrophages (51, 52). Studies regarding the mechanism of *B. burgdorferi* phagocytosis have focused primarily on MyD88-mediated signals, including PI3K activity and demonstrated that a substantial amount of *B. burgdorferi* phagocytosis is MyD88-depenendent. Nevertheless, macrophages from MyD88-deficient mice still possess detectable phagocytic capacity, demonstrating that MyD88 dependent and independent phagocytosis events are involved. However, the phagocytic receptors involved in the internalization of *B. burgdorferi* have not been fully identified.

Complement activation and bacterial opsonization

The complement system is a complex and critical component of the innate immune response to pathogens. It is comprised of serum proteins and cell surface receptors that are involved in the early detection of pathogens, such as *B. burgdorferi* (53). Complement mediated destruction of organisms involves the formation of pores in the cellular membrane by the membrane attack complex (MAC) and results in the lysis of the organism. Complement activation occurs *via* three different pathways: classical (antigen antibody-mediated), lectin and alternative (pathogen surface) pathways. All three pathways converge at the level of C3 convertase, which is a protease responsible for the cleavage of C3 into C3a and C3b. *B. burgdorferi* is able to activate both the classical and alternative pathways (54), thus C3b can bind to the surface of bacteria and facilitate internalization of the spirochete by opsonization or C3b can bind C5 convertase to facilitate MAC formation and lysis of the bacteria by depositing downstream components into the cell wall. *B. burgdorferi sensu lato* group have evolved mechanisms that enable them to evade complemented-mediated lysis,

such as expression of complement regulator-acquiring surface proteins (CRASPs). CRASPs act as binding sites for the complement inhibitor factor H and factor H-like protein (FHL-1) (55-57) and cleave bound serum complement protein C3b into the serum opsonin inactivated C3b (iC3b).

Complement Receptor 3

Complement receptor (CR) 3 also known as Mac-1 or $\alpha_M\beta_2$ integrin is a type I membrane glycoprotein comprised of α and β subunits, CD11b (165kD) and CD18 (95kD) respectively. The heterodimeric protein is expressed on phagocytic and natural killer (NK) cells. The integrin is a member of the leukocyte-restricted β_2 family that shares an identical β subunit (CD18) that is non-covalently linked to one of four α subunits: LFA-1 (CD11a/CD18), CR3 (CD11b/CD18), CR4 (CD11c/CD18) and $\alpha_D\beta_2$. α_M and β_2 are derived from nonlinked genes on the human chromosomes 16 and 21 as well as the mouse chromosomes 7 and 10, respectively. CR3 acts as an intercellular adhesion molecule, in addition to a membrane receptor with transmembrane signaling ability. The molecular structure contains two functional domains on the CD11b subunit. At the N-terminus, an inserted region of 200 amino acids that is unlike the typical integrin structure is known as the I-domain. ICAM-1, iC3b and fibrinogen, known CR3 protein ligands have been shown to interact with the I-domain of CR3 (58). The lectin-like domain (C-lectin) is located at the C-terminal end near the transmembrane domain of CD11b and allows the binding of polysaccharides from bacteria and yeast, such as filamentous hemagglutinin (FHA) of *Bordetella pertussis* and zymosan of *Saccharomyces cerevisiae*, promoting phagocytosis and cytotoxic degranulation (59). This domain is also known to interact with GPI-anchored

proteins, such as CD87 (uPAR) and CD14 (60, 61). CR3 is sufficient to internalize microorganism and particles such as *Bacillus anthracis* spores in the absence of co-receptors (62). Importantly, human neutrophils and Chinese hamster ovary (CHO) cells expressing CR3 have the ability to bind non-opsonized *B. burgdorferi* as well as the spirochetal outer surface proteins, OspA and OspB; however, the contribution to internalization of the bacteria remains unclear (63-65).

Integrins, such as CR4 and CR3 are expressed on the surface of cells in a low affinity conformation (66, 67). Upon generation of "inside-out" signals, the transmembrane domains of the integrin undergo a change to a high affinity conformation (68-70). The activation of CR3 changes ligand-binding specificity and affinity, which can enhance CR3-mediated phagocytosis. CD14 in combination with TLR2 can generate inside-out signals that result in the activation of CR3 (71, 72). For example, *Mycobacterium bovis* uptake is promoted through inside-out signaling, involving CD14, TLR2 and PI3K (71). Inside-out signals can also emanate from additional receptors, such as CD44 via the small GTPase, Rap1 (73) FcγR via PI3K (74) and TLRs (75).

CD14

CD14 is a 53-55 kDa glycosylphosphatidylinositol (GPI)-anchored membrane protein expressed on the surface of monocytes and macrophages at high levels, and on granulocytes at low levels. Besides a membrane bound form, CD14 can also be present as a soluble protein in serum. CD14 cooperates with several TLRs, such as TLR2, 3, 4, 7, 8 and 9 (26, 76-78) to mediate activation of the innate immune response in response to a number of bacterial products other than LPS, for example, *Staphylococcus aureus, Mycobacterium*

tuberculosis and *B. burgdorferi* (79-83). The role of CD14 for *B. burgdorferi* lipoprotein signaling has been extensively studied (82, 84). However, neither TLR2 nor CD14 are involved in the internalization of *B. burgdorferi* (33, 85). CR3 can function as a transmembrane signaling adaptor for GPI-anchored protein, such as CD14 and Urokinase-type plasminogen activator receptor (uPAR), as they lack a transmembrane domain of their own (60, 61). Moreover, GPI-anchored proteins have the ability to translocate receptors, like CR3 and TLR4 to lipid rafts (83, 86) and the disruption of the interaction results in diminished function (60, 87).

Significance

A large amount of research has focused on the notion that the activation of phagocytic cells occurs primarily via surface TLR signaling and that the response to isolated PAMPs mimic those elicited by whole organisms. However, reports have demonstrated that the response of innate immune cells to whole microorganisms is much more complex than the mere sum of TLR-PAMP interactions and that both the quantity and quality of the response requires the phagocytosis of these microorganisms (88-92). Similarly, the induction of a complete proinflammatory response to *B. burgdorferi* requires the internalization of the spirochete (26, 32, 52, 93). In spite of extensive research, no phagocytic receptor has been identified until recently. Our laboratory demonstrated that CR3 is a phagocytic receptor for *B. burgdorferi*. In RAW264.7 cells, a macrophage-like cell line, a blocking mAb against CD11b inhibited the phagocytosis of *B. burgdorferi* in a dose-dependent manner. Similarly, macrophages from CD11b-deficient mice showed a diminished phagocytic ability compared to controls. However, when CR3 alone is expressed in CHO cells, CR3 was insufficient for

the internalization of *B. burgdorferi* and therefore, the molecular mechanisms regulating the phagocytosis of *B. burgdorferi* remain largely unknown.

The aim of this study was to identify the mechanism by which CR3-mediated internalization of *B. burgdorferi* occurs and understand the role of MyD88 signaling on integrin activation and phagocytosis of the spirochete.

Pathogenic Species (*B. burgdorferi senu lato*)	Tick vector	Location
B. burgdorferi sensu stricto	*I. scapularis, pacificus* & *ricinus*	NE, NC, & W USA, Europe
B. garinii	*I. ricinus, I. persulcatus*	Europe & Asia
B. afzelii	*I. ricinus, I. persulcatus*	Europe & Asia

Table 1.1. Pathogenic *Borrelia*, corresponding vectors and geographic location

B. burgdorferi sensu lato is comprised of three genospecies of *B. burgdorferi* that causes human Lyme disease. There are additional species of *Borrelia* that have been identified but are non-pathogenic or minimally pathogenic. *B. burgdorferi sensu stricto* is the causative agent of Lyme disease in North America.

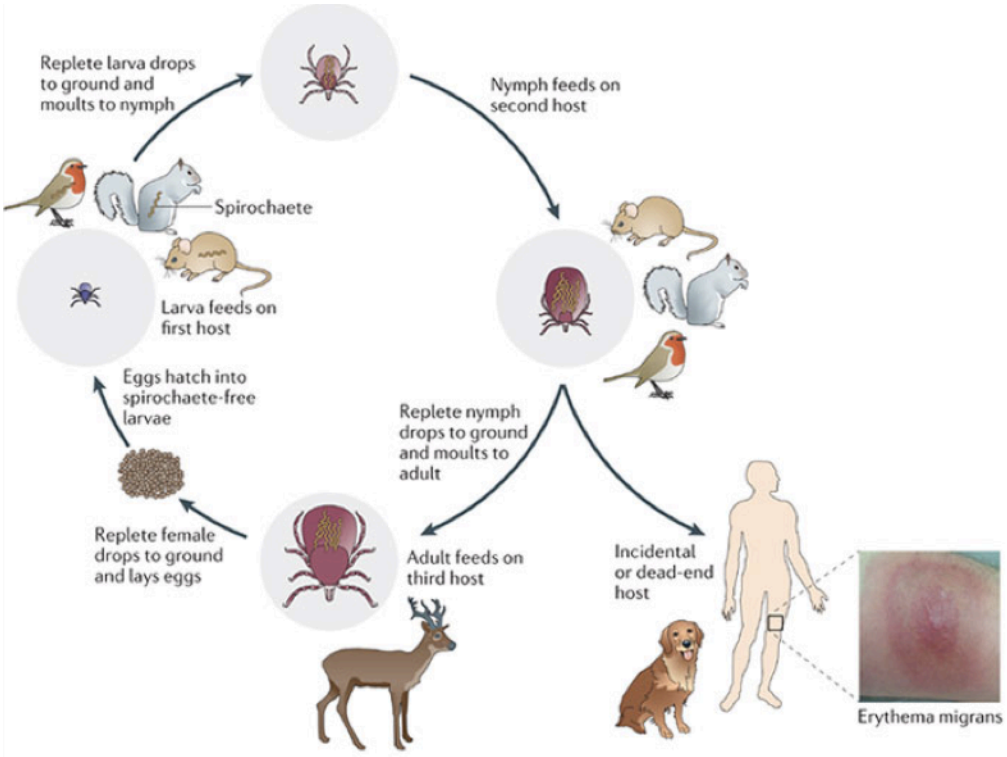

Figure 1.1. Enzoonotic cycle of *B. burgdorferi*

The life cycle of *Ixodes scapularis* requires two years. The larva hatch in early spring and obtain their first bloodmeal by feeding on birds and small rodents, such as *Peromyscus leucopus*, which can serve as reservoirs of *B. burgdorferi*. Larvae then molt into nymphs during late spring or early summer. Nymphs feed on a second host, such as small mammals or humans, allowing the transmission of the spirochete to the mammalian host. Nymphs molt into adult ticks in the fall, feeding and mating on large animals such as deer. In early spring adult females lay their eggs to complete their two-year life cycle. This figure is reproduced, with permission by Ref (94).

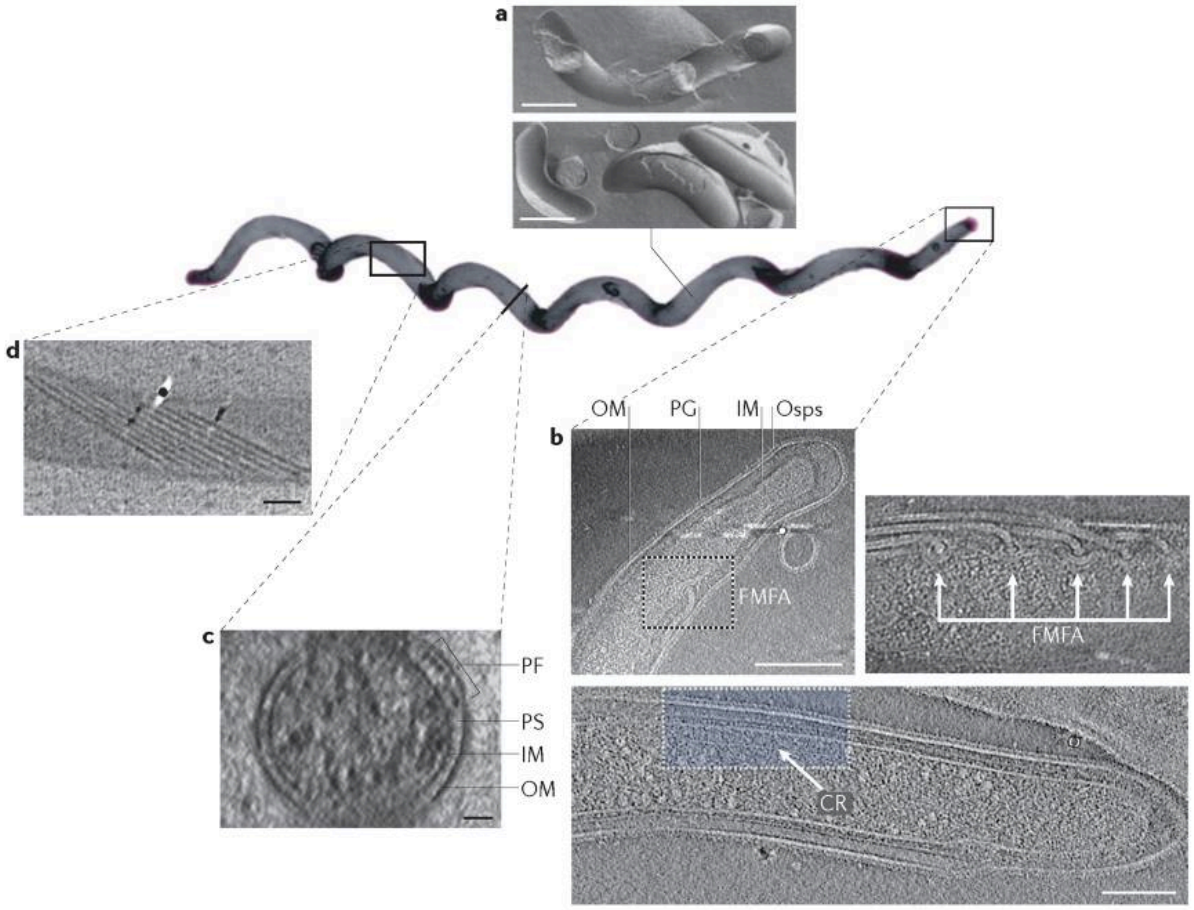

Figure 1.2. The morphological characteristics and structure of *B. burgdorferi*.

B. burgdorferi is a vigorously motile spirochete due to the periplasmic flagella, which spans the length of the spirochete between the peptidoglycan layer and outer membrane, originating from either end of the bacteria. (A) Freeze-fracture electron micrographs showing the convex and concave leaflets of the inner membrane (IM) and outer membrane (OM). Scale bars represent 500 nm. (B) Cryoelectron tomograms of the ends of borrelial cells showing IM, OM, peptidoglycan (PG), flagellar motor and filament assemblies (FMFA), chemoreceptor arrays (CR) and an external layer comprising Osps. Upper scale bar represents 1 μm, lower scale bar represents 100 nm. (C) Cryoelectron tomographic cross-section showing the IM, OM, periplasmic space (PS) and periplasmic flagella (PFs). Scale bar represents 50 nm. (D) Longitudinal cryoelectron tomographic slice showing a ribbon of nine flagellar filaments wrapping around the IM in a right-handed helix important for the characteristic shape of *B. burgdorferi* and its invasiveness into target tissues and organs by rotating around the protoplasmic cylinder. Scale bar represents 200 nm. This figure is reproduced, with permission by Ref (94).

CHAPTER II

CD14 COOPERATES WITH CR3 TO MEDIATE PHAGOCYTOSIS OF *BORRELIA BURGDORFERI*

Introduction

Phagocytosis is critical for the clearance of *B. burgdorferi* as well as the production of a robust proinflammatory response. Studies performed in our laboratory demonstrated CR3 to be the first known phagocytic receptor for the spirochete; however, CR3 alone is insufficient to internalize *B. burgdorferi*. CD14 has been demonstrated to operate as a co-receptor with many receptors, such as TLR2 (71, 72) to enhance phagocytosis, making CD14 an enticing candidate to cooperate with CR3 and mediate the internalization of *B. burgdorferi*.

Results

CR3 is a phagocytic receptor of *Borrelia burgdorferi*

Since blocking of CD11b in RAW264.7 cells reduced phagocytosis of *B. burgdorferi*, we aimed to further demonstrate that CR3 is a phagocytic receptor for *B. burgdorferi*. We examined the phagocytic capacity of CD11b-deficient and wild-type bone marrow derived macrophages (BMMs) with increasing multiplicity of infection (m.o.i.) of GFP-expressing *B. burgdorferi*. CD11b-deficient macrophages showed a decreased phagocytic activity compared to wild-type BMMs (Fig. 2.1A). CD11b deficiency did not abrogate the capacity of macrophages to phagocytose *B. burgdorferi,* which was most evident at higher m.o.i. (Fig.

2.1A). The analysis by confocal microscopy of wild-type BMM confirmed the colocalization of CD11b with GFP-containing phagosomes. However, phagosomes with spirochetes that did not contain the integrin were also evident (Fig. 2.1B). These data demonstrate that CR3 is the first identified phagocytic receptor for *B. burgdorferi* and that additional unidentified receptors also participate in the internalization of the spirochete.

We next preformed an *in vivo* phagocytosis assay (95). We injected 10^7 spirochetes intraperitoneally into CD11b-deficient and wild-type mice. The infiltrating cells were collected by peritoneal lavage after 6 hours, stained for F4/80, a macrophage specific marker, and analyzed by flow cytometry. CD11b-deficient macrophages contained lower levels of GFP-expressing *B. burgdorferi* than wild-type cells (Fig. 2.1C). The difference observed was not due to a defect in macrophage migration to the injection site because the percentage of $F4/80^+$ cells did not vary between wild-type and CD11b-deficient mice (21.1% ± 1% and 20.2% ± 3.1% respectively). Together these data demonstrate that CR3 is a phagocytic receptor for *B. burgdorferi*.

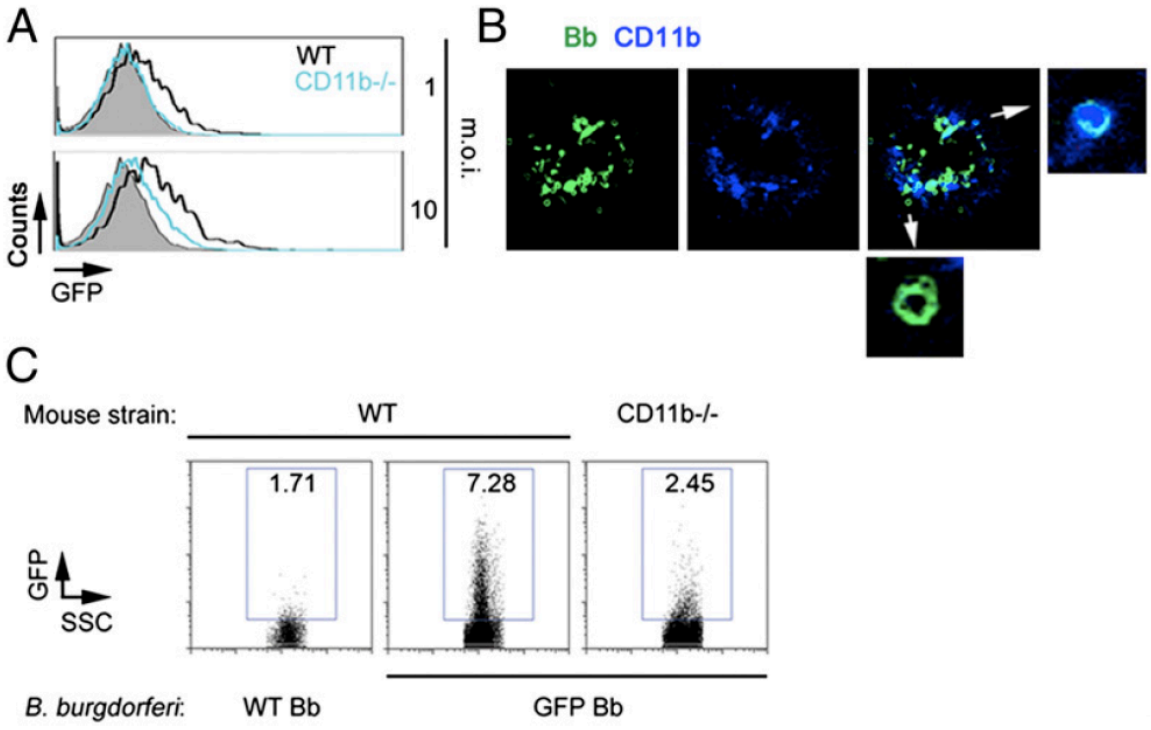

Figure 2.1. CR3 deficiency results in diminished phagocytosis of *B. burgdorferi*.

(A) Phagocytosis of Bb914 by BMMs generated from CD11b-deficient mice (blue histogram) or B6 controls (black histogram). The 4 °C binding control is represented by the grey histograms. The cells were tested at m.o.i. of 1 (top graph) and 10 (bottom graph). (B) Confocal micrograph of a wild type BMM showing colocalization of Bb914 (green) and CD11b (blue). The small panels represent internalized *B. burgdorferi* (arrows) that displayed presence or absence of colocalization with CD11b. (C) *In vivo* phagocytosis of *B. burgdorferi* by CD11b-deficient and wild-type B6 mice injected intraperitoneally with 10^7 spirochetes. A B6 mouse was also injected with non-GFP (WT) *B. burgdorferi* to control for migration of inflammatory cells into the peritoneum. The peritoneal lavages were analyzed after 6 h by flow cytometry. Shown are representative results for a total of three CD11b-deficient and three control B6 mice.

Complement enhances phagocytosis of *B. burgdorferi* in a C3-dependent manner

The previous results were performed in the absence of active complement, indicating that CR3 is able to directly interact with *B. burgdorferi* antigens and mediate its phagocytosis. However, the alternative and lectin complement pathways can enhance phagocytosis by coating the surface of bacteria with opsonins, such as iC3b. Since CR3 binds iC3b and mediates the opsonization-dependent phagocytosis of microorganisms, we investigated the role of complement-mediated opsonization in the phagocytosis of *B. burgdorferi*. We incubated RAW264.7 cell with 10% C3-deficient serum (C3-/-) or active normal mouse serum (NMS) and GFP-expressing *B. burgdorferi*. The presence of normal serum significantly enhanced the phagocytic uptake of the spirochete in a C3-dependent manner, since C3-/- serum did not enhanced the phagocytic capacity of RAW cells (Fig. 2.2A & 2.2B). These results were confirmed using primary macrophages obtained from wild-type mice (Fig. 2.2A & 2.2B). Additional experiments performed in our lab, in which CD11b was blocked with a specific mAb (clone: M1/70), reduced serum-mediated enhancement to the same level as cells in the absence of serum (data not shown), demonstrating that the increased phagocytosis observed in the presence of sera was CR3 dependent. Our results indicate that complement-mediated opsonization of *B. burgdorferi* is able to increase the phagocytosis by macrophages dependent on the serum factor C3.

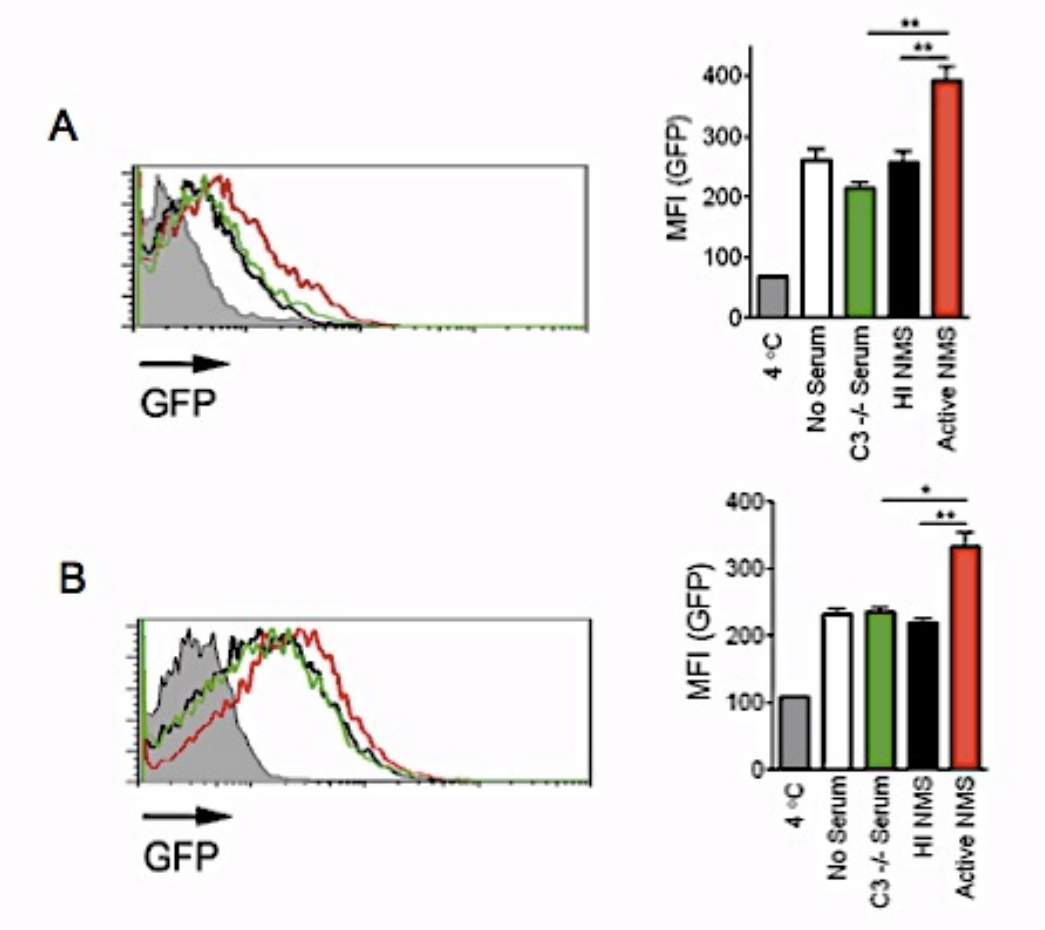

Figure 2.2. Normal, but not C3-deficient sera, increases the phagocytosis of *B. burgdorferi* by macrophages.

(A) RAW264.7 cells and (B) BMMs were incubated with GFP *B. burgdorferi* at an m.o.i. of 25 for 6 h, in the presence of heat-inactivated (black histogram), normal (red histogram) and C3-deficient mouse sera (green histogram). The gray histogram indicates the 4°C binding control. Cells were analyzed by flow cytometry (left panel); calculated MFI of GFP and values expressed in a bar graph (right panel). The results are the average ± SE of one experiment and is representative of two performed in triplicate. *, Student's *t* test, $p < 0.05$ and **, Student's *t* test, $p < 0.001$.

CspA and OspE protect against serum-mediated phagocytosis

B. burgdorferi is capable of disseminating and persisting in various tissues of the host suggesting that *B. burgdorferi* has developed mechanisms to evade innate immune responses. *B. burgdorferi* lipoproteins, CspA, CspZ and OspE-related proteins are collectively referred to as complement regulator-acquiring surface proteins (CRASPs) and have been shown to bind Factor H (FH) and FH-like proteins (55, 56, 96), which are negative regulators of the alternative complement pathway. Both CspA and OspE inhibit complement to evade spirochetal killing (97, 98). However, CspZ is not exposed to the surface and is not required for serum resistance or infection (99). To elucidate the contribution of CspA in the serum-mediated phagocytosis of the spirochete, we utilized a GFP-expressing B31 stain of *B. burgdorferi* in which *cspa* was interrupted by insertion of a streptomycin resistance cassette. BMMs from B6 mice were incubated with the CspA mutant (CspA-) spirochete, 10% HI or NMS and analyzed by flow cytometry. The *cspa* gene was complemented (CspA +) to confirm that the phenotype observed was the result of the loss of the lipoprotein encoded by *cspa*. The uptake of the CspA- spirochetes was significantly higher than CspA+ *B. burgdorferi* in the presence of 10% NMS (Fig 2.3A & 2.3B). However, there was no difference between the two strains of spirochetes when incubated with 10% HI serum (Fig. 2.3A). Moreover, the phagocytic capacity of human monocytes (hMon) was significantly higher for the mutant spirochete (Fig 2.3C). These data demonstrate that *B. burgdorferi* CspA protects the spirochete from serum-mediated phagocytosis.

We also evaluated the contribution of *B. burgdorferi* outer surface protein E (OspE) in opsonin-mediated phagocytosis. OspE was overexpressed in CspA-deficient spirochetes

(100). BMM and hMon were cultured with 10% heat inactivated or active serum. The overexpression of OspE resulted in a significant reduction in the ability of both BMMs and human monocytes to phagocytose the spirochete, compared to spirochetes containing the vector control (Fig 2.4A & 2.4B); these results show that both CspA and OspE allow the spirochete to evade complement-mediated opsonization and phagocytosis.

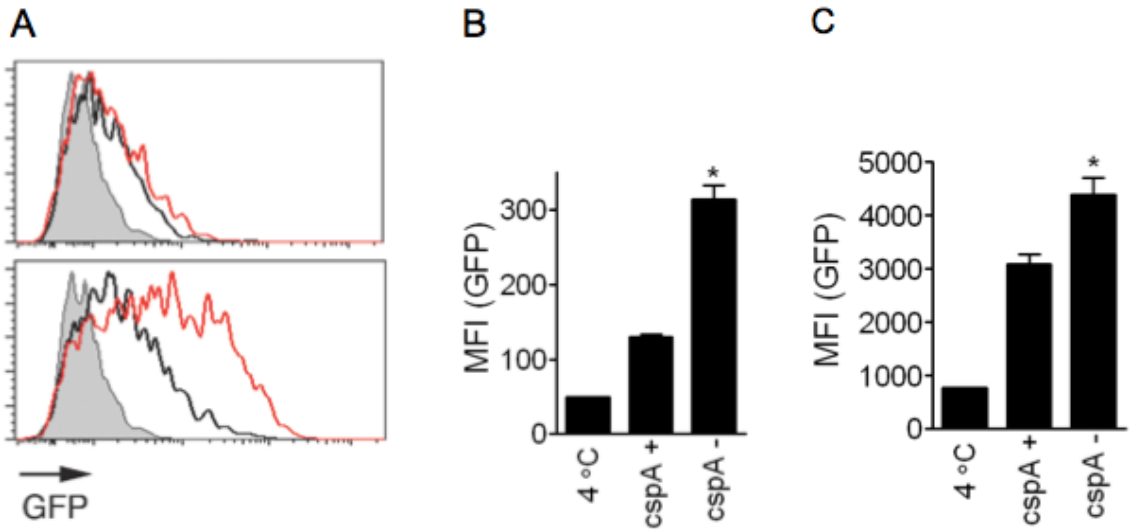

Figure 2.3. CspA protect against serum-mediated phagocytosis.

(A) BMMs were incubated with the GFP-expressing *B. burgdorferi* B31 CspA mutant (red histogram) or the CspA complement (black histogram), in the presence of heat-inactivated (top panel) or 10% normal mouse sera (bottom panel). The experiments were performed at an m.o.i. of 25 and a 4 h period of incubation. (B) BMM and (C) hMon phagocytic capacity for CspA mutant and complement *B. burgdorferi* with 10% active mouse or human sera, respectively, were represented by the MFI of GFP. *, Student's *t* test, $p < 0.05$.

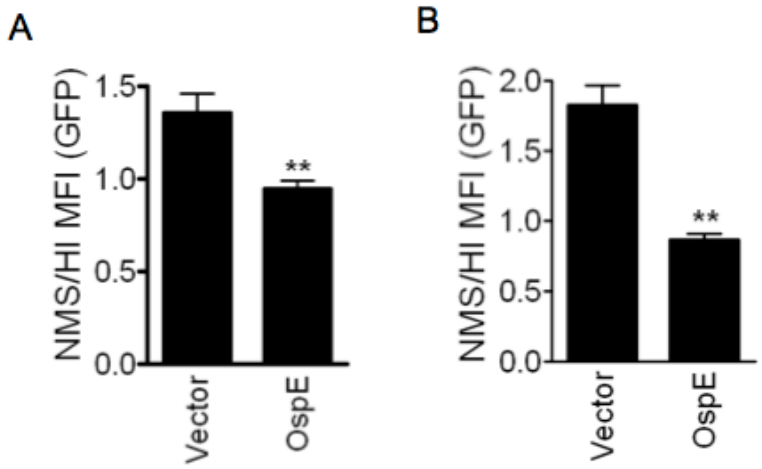

Figure 2.4. Expression of OspE reduces serum-mediate phagocytosis of *B. burgdorferi*.

CspA-deficient, GFP *B. burgdorferi* B31 containing a plasmid control (gfp-pSP1G) or complemented with the *ospE* gene (OspE-gfp-pSP1G) were used in phagocytosis assays at an m.o.i. of 25 for 4h with (A) BMMs or (B) hMon in the presence of heat inactivated or active sera. The active serum MFI was normalized to the HI serum MFI to account for the different levels of GFP expression by both strains (data not shown). The results are the average ± SE of one experiment and is representative of two experiments performed in triplicate. **, Student's *t* test, $p < 0.001$.

CD14 cooperates with CR3 during phagocytosis of *B. burgdorferi*

Studies preformed in our laboratory demonstrated that CHO cells stably expressing human CR3 lack the ability to internalize *B. burgdorferi*. These results could be the result of a functional defect of the ectopically expressed CR3 or because CR3-dependent phagocytosis of *B. burgdorferi* requires a co-receptor. To evaluate the phagocytic ability of CHO-CR3 cells, we incubated the cells with zymosan$_{488}$ particles, which only require CR3 for internalization (101). The cells were analyzed by Apotome fluorescence microscopy to confirm that the ectopically expressed CR3 in the CHO cell line is functional and the cells possess phagocytic capacity (Fig. 2.5A). Therefore, our results implied that CR3 requires a co-receptor for the phagocytosis *B. burgdorferi*. The GPI-anchored protein, CD14 has been shown to enhance CR3-mediated phagocytosis of several pathogens and particles such as *Bacillus anthracis* spores and *Mycobacterium kansasii* (62, 102). We utilized a CHO-CR3 cell line expressing CD14 (CHO-CR3/CD14) (103) to analyze their phagocytic capacity against *B. burgdorferi*. CHO-CR3/CD14 cells were readily able to phagocytose the spirochete (Fig. 2.5A) in a CR3-dependent manner, since preincubation with the mAb M1/70 resulted in the reduced uptake of *B. burgdorferi* when compared to cells incubated with the isotype control (Fig. 2.5B).

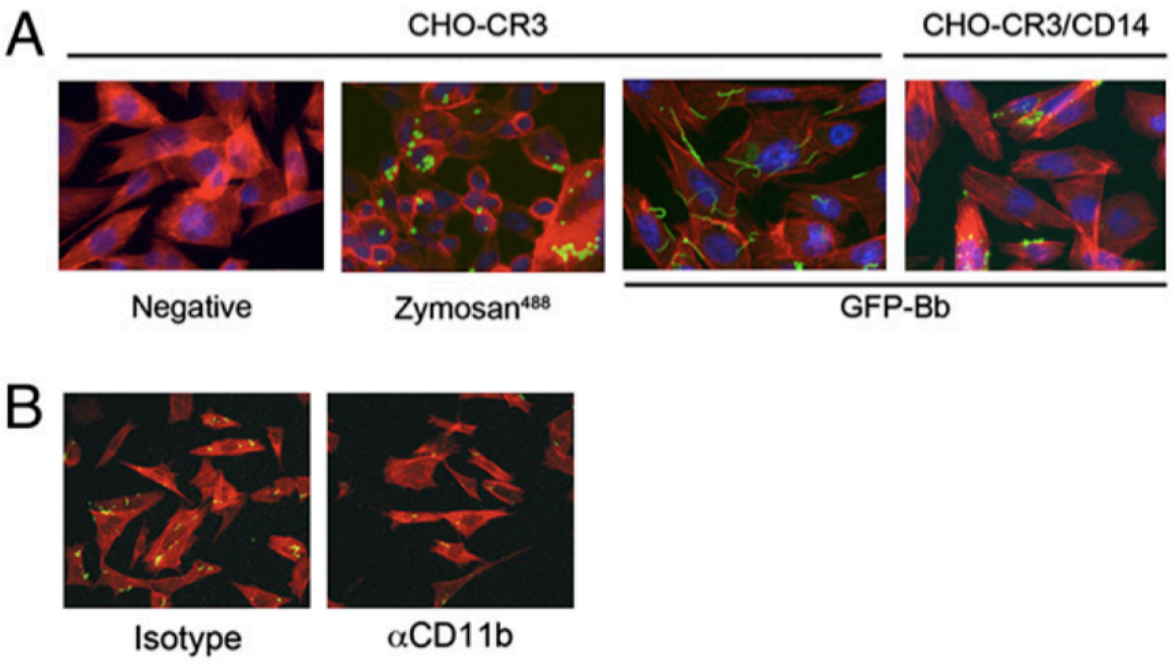

Figure 2.5. CD14 cooperates with CR3 to promote phagocytosis of *B. burgdorferi*.

(A) CHO-CR3 and CHO-CR3-CD14 cells were grown in eight-well chamber slides and incubated with Zymosan labeled with Alexa Fluor 488 (m.o.i. = 5) or Bb914 (m.o.i. = 25) for 4 h. The cells were washed, fixed, permeabilized and stained with phalloidin Alexa Fluor 594, followed by analysis by Apotome fluorescence microscopy. (B) CHO-CR3/CD14 cells grown in chamber slides were incubated with Bb914 (m.o.i. = 25) for 4 h in the presence of M1/70 mAb or an isotype control. The cells were fixed, stained with phalloidin Alexa Fluor 594 and analyzed by confocal microscopy.

CD14 does not contribute to the binding of *B. burgdorferi*

To investigate whether CD14 cooperates with CR3 by participating in the binding of *B. burgdorferi*, we incubated CHO-CR3 and CHO-CR3/CD14 cells with increasing m.o.i. of spirochetes and analyzed their binding capability by flow cytometry. The two cell lines were able to bind the bacteria equally (Fig. 2.6A). We next pretreated CHO-CR3/CD14 cells with 10μg/ml of the human CD14 blocking antibody or an isotype control (104) and flow cytometry was used to compare the internalization of the spirochetes (Fig 2.6B). Treatment with the blocking antibody resulted in no difference in the CHO-CR3/CD14 cells ability to phagocytose *B. burgdorferi* when compared to the cells treated with the isotype control. We verified these results using a mouse-specific antibody and RAW264.7 cells (Fig. 2.6C). These data indicate that CD14 does not contribute to the binding of *B. burgdorferi*.

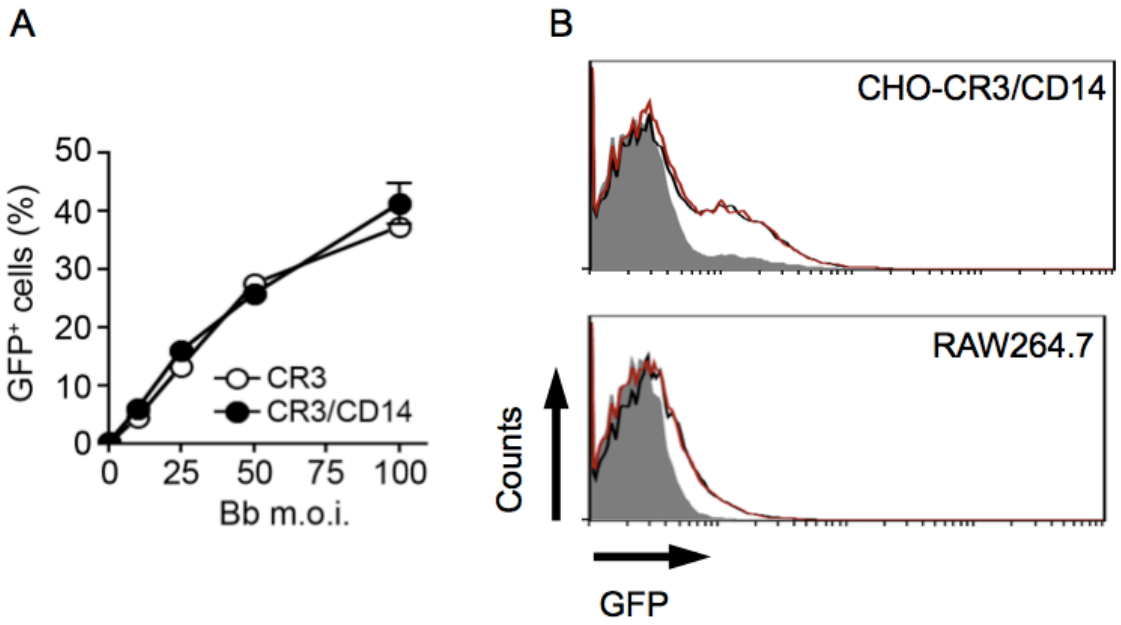

Figure 2.6. CD14 does not contribute to *B. burgdorferi* binding.

(A) CHO-CR3 (open circles) and CHO-CR3/CD14 (solid circles) were incubated with increasing m.o.i. of Bb914 and then analyzed by flow cytometry. (B) CHO-CR3/CD14 (top panel) and RAW264.7 (bottom panel) were pre-incubated with 10μg/ml of CD14 blocking antibody (Red histogram) or isotype control (Black histogram), then Bb914 (m.o.i. = 25) for 4 h and analyzed by flow cytometry. (A) The results represent the mean percentage of GFP+ cells ± SE for three independent experiments. (B) The results are representative of two independent expreiments performed in triplicate.

CR3-mediated phagocytosis of *B. burgdorferi* requires its translocation to the lipid rafts

CD14 is present in cholesterol rich domains on the plasma membrane and induces the specific assembly of additional receptors to initiate signaling cascades (85, 105). Our results suggested that CD14 interacts with CR3 during *B. burgdorferi* phagocytosis (Fig 2.7A). We confirmed the colocalization of CD11b and CD14 by confocal microscopy in BMMs in the presence as well as the absence of *B. burgdorferi* (Fig. 2.7A). To assess whether CR3 translocates to membrane microdomains upon interaction with *B. burgdorferi*, we performed a sucrose density gradient assay with RAW264.7 cells that had been incubated with *B. burgdorferi* at an m.o.i. of 25. The gradient was fractionated, precipitated and analyzed by immunoblotting. CD11b co-localized with CD14 in the lipid raft fractions of the gradient regardless of the activation status of the cells. However, we observed a degree of CD14 reorganization and an increased level of the protein upon stimulation with *B. burgdorferi* (Fig. 2.7B).

Lipid rafts are rich in ganglioside GM1 that readily bind cholera toxin subunit B (CTxB) making it a useful method for their detection (106). We analyzed CD11b and CTxB staining by confocal microscopy in RAW264.7 cells in the presence or absence of *B. burgdorferi*. CD11b colocalized with CTxB under both conditions (Fig. 2.7C). Moreover, *B. burgdorferi* were attached to the surface of the macrophage in lipid rich regions stained with CTxB (Fig. 2.7C).

To determine the contribution of lipid rafts to the internalization of *B. burgdorferi*, we analyzed RAW264.7 cell phagocytic ability in the presence and absence of methyl-β-cyclodextran (MβCD), a lipid-sequestering compound that disrupts the cholesterol component of the lipid rafts (107). RAW264.7 cells were incubated with 5mM MβCD, a

concentration that does not affect cell viability, prior to the phagocytosis assay. The disruption of lipid rafts revealed a partial reduction in the phagocytic capacity of RAW264.7 cells (Fig. 2.7D). CHO-CR3/CD14 cells were also treated under the same conditions, which resulted in an almost complete abrogation of *B. burgdorferi* internalization (Fig. 2.7D). These data indicate that CR3 phagocytosis requires the translocation of CR3 to membrane microdomains.

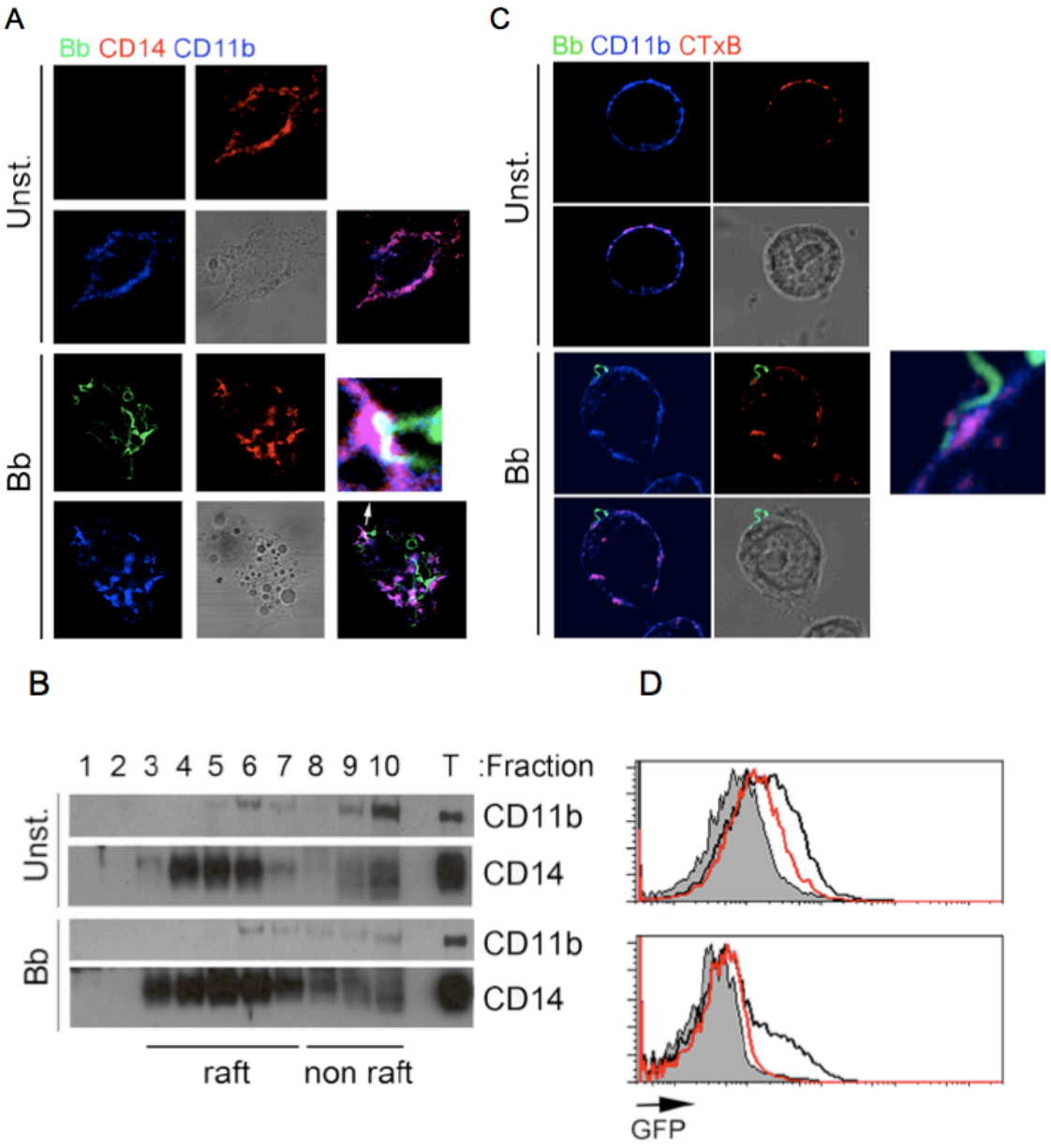

Figure 2.7. CR3-mediated phagocytosis of *B. burgdorferi* requires the translocation of the integrin to lipid rafts.

(A) Co-localization of CD11b and CD14 in BMMs stimulated with Bb (m.o.i.= 10) or cells that were left unstimulated. The cells were incubated with Bb for 1 h, fixed and stained with anti-CD14 (red) and anti-CD11b (blue) Abs. Co-localization of CD14 and CD11b is noted in purple. Triple co-localization with GFP is shown in white. (B) RAW264.7 cells were incubated for 1 h with Bb (m.o.i. = 25), lysed and layered onto a sucrose gradient. The gradients were separated by ultracentrifugation for 20 h following which 10 fractions of 100 µl were collected. The fractions were precipitated with tricholoroacetic acid, run on a SDS-PAGE, transferred to nitrocellulose membranes and immunoblotted with anti-CD11b and

anti-CD14 Abs. Fraction numbers from the top are indicated. T: whole lysates (25 μg). (C) Confocal micrographs showing CD11b localization to lipid rafts. RAW264.7 cells were incubated with Bb914 (lower panels) or left unstimulated (upper panels) for 30 min. The cells were washed, fixed and stained with an anti-CD11b Ab (blue) and CTxB (red). Colocalization of CD11b and CTxB staining is indicated by the purple color in the small panel. (D) RAW264.7 cells (Top panel) or CHO-CR3/CD14 (Bottom panel) were preincubated with 5 mM of MβCD (red histogram), followed by incubation with Bb914 (m.o.i. = 25) for 2 hours. The cells were then analyzed by flow cytometry. Control cells (black histogram) were left untreated. The results presented are representative of 3-5 individual experiments.

Engagement of the C-Lectin domain in CR3 is sufficient to internalize *B. burgdorferi*

CR3 contains an I-domain that binds to opsonized bacteria and a C-lectin domain that can bind sugars such as β-Glucan and GPI-anchored proteins. To assess whether CR3 crosslinking upon engagement of the C-lectin domain was sufficient for the phagocytosis of *B. burgdorferi*, we evaluated the involvement of the C-lectin domain on the uptake of the spirochete. RAW 264.7 cells were incubated with *B. burgdorferi* (m.o.i. = 25) and β-Glucan from different origins for 4 hours. The treatment with *S. cerevisiae* β-Glucan enhanced the phagocytosis of the spirochetes (Fig. 2.8A) suggesting that interaction with the C-lectin domain may be sufficient for CR3 crosslinking and phagocytosis.

We also treated CHO-CR3 cells lacking CD14 with *S. cerevisiae* β-Glucan during incubation with *B. burgdorferi* (m.o.i. = 10) and analyzed the cells by confocal microscopy. We observed that the bacteria were internalized in the same manner as the CHO-CR3/CD14 cells (Fig. 2.8B). These data show that CR3-mediated phagocytosis of *B. burgdorferi* requires the engagement of the C-lectin domain of the integrin.

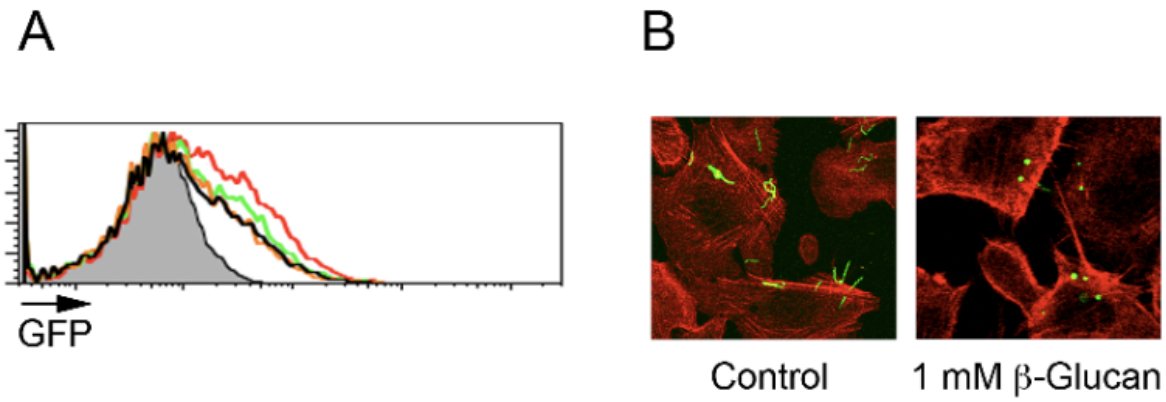

Figure 2.8. Engagement of C-lectin domain is sufficient to internalize *B. burgdorferi*.

(A) RAW264.7 incubated with 1mM barley β-Glucan orange histogram), Laminarin β-Glucan (green histogram) and *S. cerevisiae* β-Glucan (red histogram) and Bb914 (m.o.i. = 25) for 4 hours. The control cells (black histogram) were incubated with Bb914. (B) CHO-CR3 cells were incubated with 1mM *S. cerevisiae* β-Glucan and Bb914 for 4 hours. The cells were fixed, stained with phalloidin Alexa Fluor 594 and analyzed by confocal microscopy. The results presented are representative of 3 experiments preformed in triplicate.

Infection of CD11b-deficient mice results in increased cardiac inflammation and deficient bacterial control

Macrophages are critical for bacterial clearance and proinflammatory cytokine production. Our laboratory has demonstrated that macrophages deficient in CD11b have reduced ability to phagocytose *B. burgdorferi*. Given the importance of CR3 in bacterial phagocytosis (61-63, 71, 102), we assessed the contribution of CR3 during infection with *B. burgdorferi*. Wild type C57Bl/6 (WT) mice and CD11b-deficient C57Bl/6 (CD11b -/-) mice were subcutaneously injected with *B. burgdorferi* strain 297 and analyzed at 2 weeks of infection. Arthritis and carditis severity were evaluated by H&E histological analysis. CD11b-deficient mice developed similar levels of arthritis as wild type controls (Fig 2.9B). However, carditis severity in CD11b-deficient mice was significantly increased compared to controls (Fig. 2.9A). The lack of CD11b resulted in a significant increase in the percentage of infected hearts (Fig. 2.9C), as well as the geometric mean of the number for bacteria per infected heart (WT: 24, CD11b-deficient: 174 copies of spirochetal *recA* per copy of murine *actin*). These results showed that CR3 is critical for pathogen control and disease severity during infection with *B. burgdorferi*.

CD11b has been shown to be a negative regulator of TLR-triggered proinflammatory cytokines, such as TNF, involving the degradation of MyD88 and TRIFF by the E3 ubiquitin ligase (108). To determine whether the loss of the β_2 integrin plays a role in the *in vivo* proinflammatory response to *B. burgdorferi* infection, *w*e analyzed *tnf* gene expression from the cardiac tissue of infected mice by isolating total RNA for qRT-PCR. We observed that the levels of cytokine transcript were significantly increased in the absence of the integrin compared to wild type mice (Fig. 2.10A). These results correlated with the increased TNF

production by CD11b-deficient macrophages in response to *B. burgdorferi* stimulation compared to controls (Fig. 2.10B), (52). This response mimicked the increased cytokine production in response to the spirochete observed in CD14-deficient mice (109) and strongly supports a model in which GPI-anchored proteins cooperate with CR3 in the internalization of the spirochete and the modulation of cytokine expression in response to *B. burgdorferi*.

A

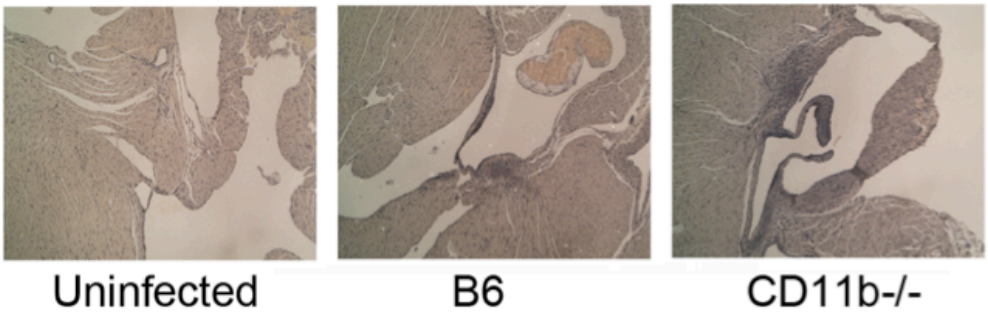

B

	Arthritis (Average ± SE)	Carditis (Average ± SE)	
WT	1.10 ± 0.16	0.32 ± 0.14	*
CD11b-/-	0.91 ± 0.19	0.82 ± 0.14	

*Student's T test, p = 0.02

C

Hearts Infected (%)	WT	CD11b-/-
Infected	44	62
Non Infected	56	38
	100	100
χ^2, p = 0.01	n = 16	n = 16

Figure 2.9. Lyme carditis in CD11b-deficient mice involves deficient control of *B. burgdorferi*.

CD11b-deficient and wild-type controls were infected with 10^5 spirochetes by s.c. injection in the midline of the back. (A and B) After being euthanized, the mice were analyzed histologically for signs of arthritis (B) and carditis (A and B). *Student's *t* test, $p < 0.05$. n = 11 in each group. (C) Percentages of hearts positive for *B. burgdorferi* recA targets by qPCR. *χ^2, $p < 0.05$. n = 16 in each group.

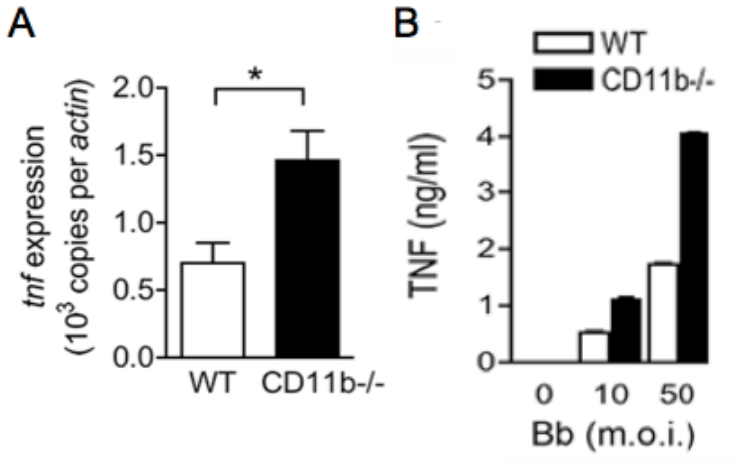

Figure 2.10. CD11b modulates the proinflammatory cytokine, TNF.

(A) The levels of *tnf* gene expression in the hearts of the infected mice were analyzed by qRT-PCR relative to *actin* levels. *Student's *t* test, $p < 0.05$. n = 11 in each group. The results represent two to three independent experiments with 5–6 mice per group. (B) TNF production by B6 and CD11b-deficient BMMs in response to *B. bu*rgdorferi stimulation. BMMs were stimulated with live spirochetes at increasing m.o.i. for 16 hours, followed by the analysis of the stimulation supernatants for TNF by ELISA.

CHAPTER III

THE ACTIVATION OF CR3 ENHANCES PHAGOCYTOSIS OF *BORRELIA BURGDORFERI* AND IS INDEPENDENT OF MYD88-INDUCED SIGNALS

Introduction

Inside-out signals can emanate from a variety of receptors such as CD14/TLR2 (71, 72) and induce the activation of integrins, like CR3. The conformational change to the integrin can enhance ligand affinity and increase phagocytosis. However, the involvement of integrin activation in response to *B. burgdorferi* has yet to be studied. Additionally, MyD88 signaling is partly required for phagocytosis of *B. burgdorferi* (33, 110) even though the signaling receptors, TLR2 and CD14 are not involved in the internalization of the spirochete (33, 85), which suggests that both MyD88-dependent and independent pathways contribute to spirochetal uptake by macrophages.

Results

Activation of CR3 enhances, but is not required for, *B. burgdorferi* uptake

Integrins, including CR3, are present on the cell surface in a low affinity conformation but can undergo conformational changes that lead to an increase in ligand affinity (111). Inside-out signals can stem from CD14/TLR2 engagement as well as other receptors such as CD44 or Fc receptors. To identify whether *B. burgdorferi* induces CR3

activation, we used an antibody clone (CBRM1/5) that specifically binds to the high-affinity conformation of the integrin. The incubation of RAW264.7 cells with live *B. burgdorferi* or 1μM Mn^{2+} resulted in the increased binding of the CBRM1/5 mAb (Fig. 3.1A). We next determined if the activation of CR3 with Mn^{2+} enhances the RAW264.7 cells' ability to phagocytose *B. burgdorferi*. We observed a dose-dependent increase in internalized spirochetes with the activation of CR3 by Mn^{2+} (Fig. 3.1B).

We then addressed the effect of *B. burgdorferi* stimulation on CR3 affinity in CHO-CR3 and CHO-CR3/CD14 cells. In both cases, the stimulation with *B. burgdorferi* failed to increase binding of CBRM1/5, while Mn^{2+} induced the expected conformational change in CR3 (Fig. 3.1C). These data show that the activation of CR3 although not required, can enhance the internalization of *B. burgdorferi*.

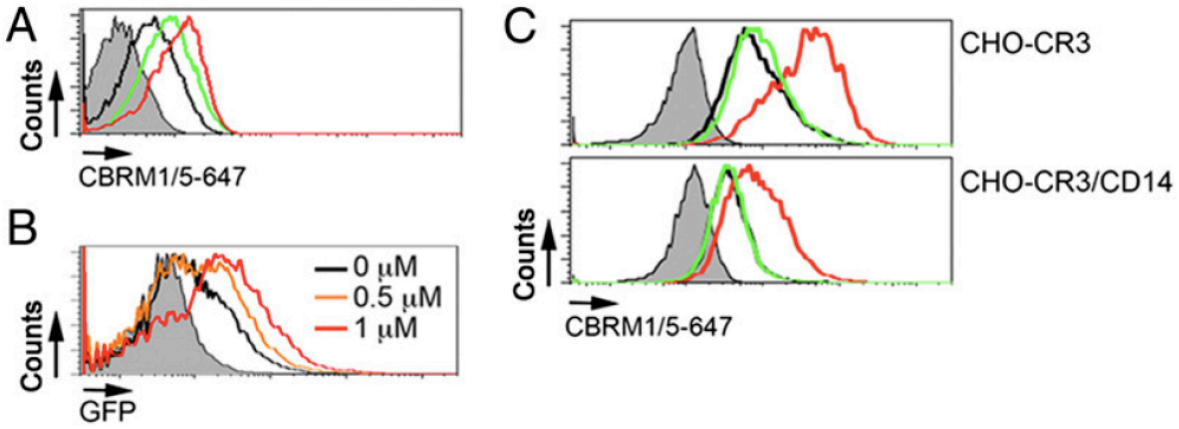

Figure. 3.1. Inside-out signals are not required for the phagocytosis of *B. burgdorferi*.

(A) RAW264.7 cells were incubated with Bb914 (m.o.i. = 25, green histogram) or MnCl2 (1 μM, red histogram), washed and stained with the mAb CBRM1/5. The cells were fixed and analyzed by flow cytometry. (B) RAW264.7 cells were incubated with increasing concentrations of MnCl2 (0.5 μM, orange histogram; 1 μM, red histogram) or left unstimulated (black histogram), washed and assessed for their phagocytic activity using Bb914 (m.o.i. = 25). (C) CHO-CR3 (upper) and CHO-CR3/CD14 cells (lower) were incubated with Bb914 (green histograms) or MnCl2 (red histograms), as before. The cells were stained with the mAb CBRM1/5, fixed and analyzed by flow cytometry.

MyD88-signals are not required for CR3-mediate phagocytosis or integrin activation

Phagocytosis of *B. burgdorferi* is partly dependent on MyD88 and PI3K signals (110). However, CHO cells lack a functional TLR2 (112), which suggests that the internalization of *B. burgdorferi* mediated by CR3 is independent of MyD88 signals. To evaluate the role of MyD88 signals in CR3-mediate phagocytosis of *B. burgdorferi*, we assessed the uptake of the spirochete by CHO-CR3/CD14 cells pretreated with a membrane-permeable MyD88-blocking peptide. The blocking peptide did not affect the internalization of *B. burgdorferi* by CHO-CR3/CD14 cells in comparison to RAW264.7 cells (Fig. 3.2A). These results were confirmed by confocal microscopy (Fig. 3.2B).

To investigate the role of MyD88-derived signals on integrin activation, we pretreated RAW264.7 cells with the MyD88-blocking peptide followed by stimulation with *B. burgdorferi*. The inhibition of MyD88 did not affect the activation of CR3 in response to the spirochete (Fig. 3.2C), suggesting that MyD88 signals are not involved in inside-out signaling leading to the activation of CR3.

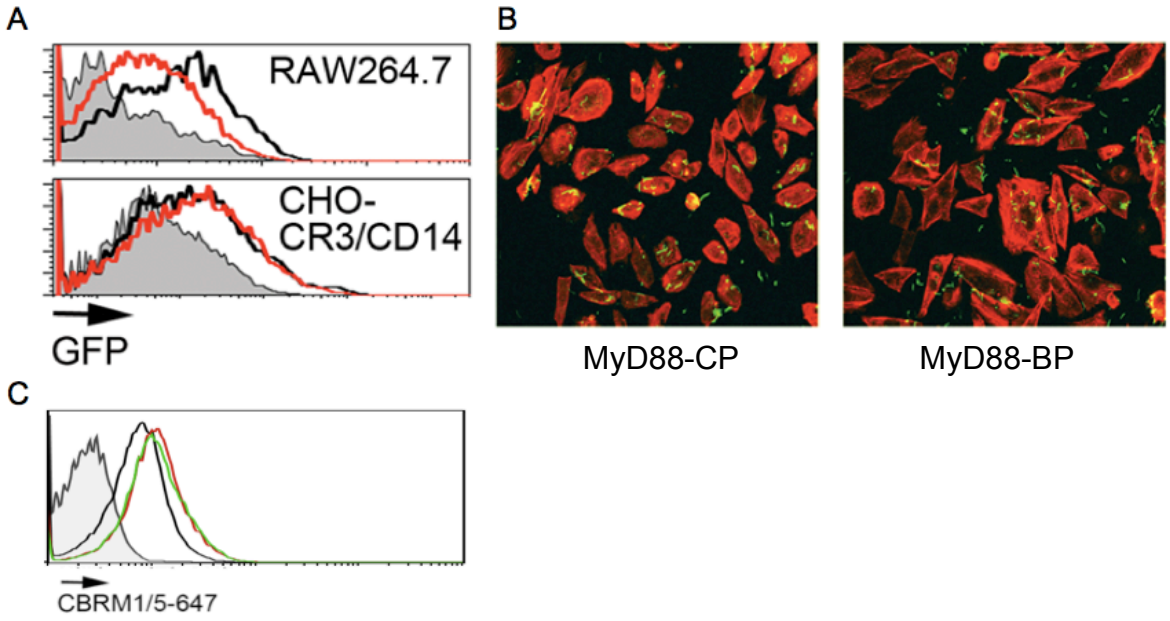

Figure 3.2. CR3-mediate phagocytosis of *B. burgdorferi* is MyD88-independent.

(A) Flow cytometric analysis of phagocytosis by CHO-CR3/CD14 (bottom panel) and RAW264.7 cells (top panel) in the presence of MyD88-BP (red histograms) or the control peptide (black histograms). The cells were pre-incubated with the peptides at 50 μM for 1 h, prior to adding Bb914 (m.o.i. = 25). (B) Confocal images of *B. burgdorferi* phagocytosis by CHO-CR3/CD14 cells in the presence of a blocking MyD88 peptide. Chamber-grown cells were incubated with 50 μM of the blocking MyD88 peptide (MyD88-BP) or a peptide control (MyD88-CP) for 1h, followed by incubation with Bb914 for 4 hours. The cells were then washed, fixed and stained with phalloidin- Alexa fluor 594. (C) RAW264.7 cells were preincubated with the peptides at 50 μM for 1 h MyD88-BP (red histogram) or the control peptide (green histogram), prior to adding Bb914 (m.o.i. = 25) Bb914 for 15 mins, then washed and stained with the mAb CBRM1/5. The cells were fixed and analyzed by flow cytometry.

CR3-mediated phagocytosis of *B. burgdorferi* is independent of PI3K signals

We analyzed the uptake of *B. burgdorferi* by CHO-CR3/CD14 cells in the presence of the PI3K inhibitors, LY294002 and wortmannin. The presence of either inhibitor did not affect the ability of CHO-CR3/CD14 cells to phagocytose *B. burgdorferi* (Fig. 3.3); however, RAW264.7 cells (Fig. 3.3) exhibited a diminished bacterial uptake in the presence of both inhibitors, as reported (110). Together these data show the in CHO cells, CD14 cooperates with CR3 independently of TLR2 and MyD88-derived signals, including PI3K activity.

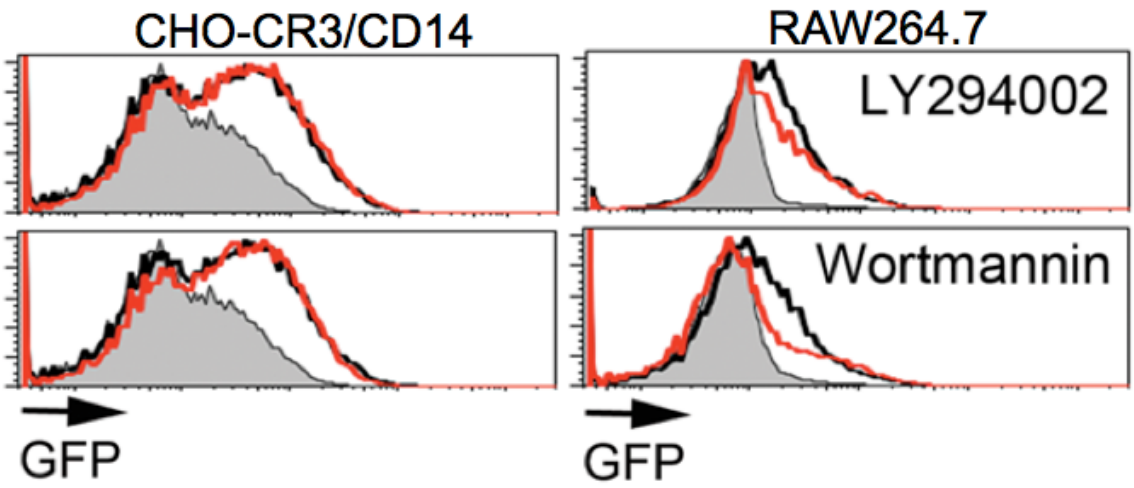

Figure 3.3. CR3-mediated phagocytosis of *B. burgdorferi* is independent of PI3K signals.

Flow cytometric analysis of phagocytosis by CHO-CR3/CD14 (left histograms) and RAW264.7 cells (right histograms). The cells were preincubated with the PI3K inhibitors, LY294002 (10 μM) and wortmannin (2 μM) (red histograms) or DMSO (control, black histograms). The cells were incubated with the inhibitors for 1 h, followed by Bb914 (m.o.i = 25). Phagocytosis was allowed to proceed for 4 h. The results are representative of at least 3 experiments performed in triplicate.

CR3 activation and CR3-mediated phagocytosis of *B. burgdorferi* is independent of Rap1 signals

CD44 has been shown to induce inside-out activation of CR3 *via* the small GTPase, Rap1 (73). However, when we incubated RAW264.7 cells with a CD44 blocking antibody, there was no difference in phagocytosis of *B. burgdorferi* when compared to isotype-treated controls (data not shown) demonstrating that CD44 does not play a role during the phagocytosis of *B. burgdorferi*. We further investigated the potential role of Rap1 in the activation of CR3. RAW267.4 cells were pretreated with the Rap1 inhibitor, GGTI-298 or DMSO, and stimulated with *B. burgdorferi*. The inhibition of Rap1 did not affect the binding of the high affinity specific antibody, CBRM1/5 to the *B. burgdorferi* stimulated RAW264.7 cells (Fig. 3.4A), demonstrating that Rap1 does not mediate the activation of CR3. However, RAW264.7 cells treated with the inhibitor displayed a reduction in their phagocytic capacity against *B. burgdorferi,* compared to DMSO-treated controls (Fig. 3.4B). Importantly, CHO-CR3/CD14 cells incubated with GTTI-298 readily internalized *B. burgdorfer*i to similar levels as the controls (Fig. 3.4C). Furthermore, RAW264.7 cells treated with GGTI-298 secreted a significantly lower level of TNF (Fig. 3.4D). These results showed that Rap1 regulates the phagocytosis of *B. burgdorferi* independently of CR3.

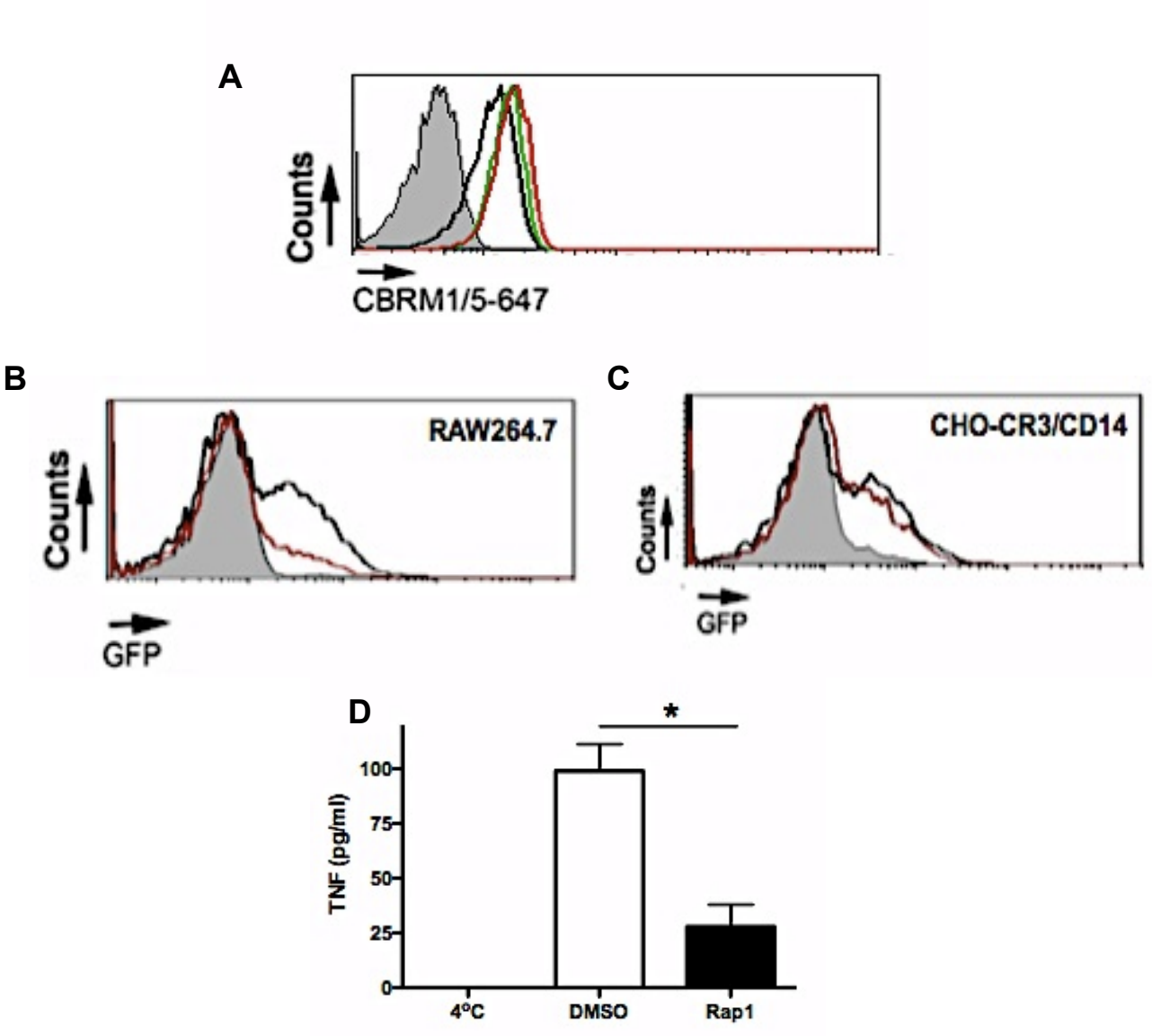

Figure 3.4. Rap1 signaling does not induce activation of CR3 and participate in CR3-mediated phagocytosis of *B. burgdorferi*.

(A) RAW264.7 cells were pre-incubated with GTTI-298 then incubated with Bb914 (m.o.i. = 10, green histogram) or DMSO (red histogram), washed and stained with the mAb CBRM1/5. The cells were fixed and analyzed by flow cytometry (B) RAW264.7 cells (C) CHO-CD3-CD14 cells were preincubated with 20μM GTTI-298 (red histogram) or DMSO (black histogram) then with Bb914 (m.o.i. = 25) for 6 hours. (D) Supernatants from experiments in B were analyzed by ELISA for TNF production.

B. burgdorferi phagocytosis is independent of p38 MAP kinase activity

p38 MAP kinase activity has been suggested to be involved in phagocytic events and the maturation of the phagosome (113). To assess the role of p38 in phagocytosis of *B. burgdorferi*, we generated transgenic (Tg) mice with repressed p38 activity in macrophages through overexpression of a dominant negative form of the kinase (Fig. 3.A) (114). BMMs generated from the Tg mice internalized GFP-expressing *B. burgdorferi* as efficiently as normal litter control (NLC) macrophages (Fig. 3.5B), indicating that the transgene did not affect the ability of the macrophage to eliminate the spirochete by phagocytosis. The cell surface protein levels of CD11b on BMMs of the Tg mice and NLC were identical (Fig. 3.5C). These results demonstrate that internalization of *B. burgdorferi* by macrophages does not require p38 MAP kinase activity.

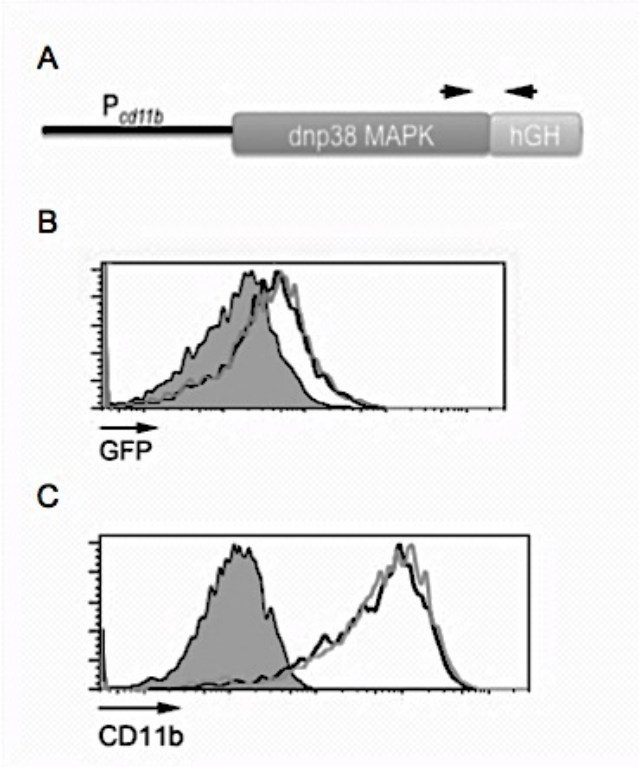

Figure 3.5. p38 MAP kinase does not regulate phagocytosis of *B. burgdorferi.*

(A) Schematic representation of the dnp38 MAP kinase gene used to generate the transgenic mice (top) showing the promoter (*cd11b*), the dnp38 gene, followed by the human growth hormone polyA/intron signal sequence. The arrows represent the localization of the primers used to detect mRNA expression in different tissues (Fig. 3.6A) plus bone marrow-derived macrophages. Primers for *actin* were used as control. (B) Phagocytosis of GFP-expressing *B. burgdorferi* by Tg (grey histogram) and NLC (black histogram) BMMs. The cells were incubated at an m.o.i of 10 for 4 h, followed by washing and their analysis by flow cytometry. The grey-filled histogram represents the 4 °C control. (C) Surface expression levels of CD11b on Tg (gray histogram) and NLC (black histogram) BMMs, determined by flow cytometry.

Validation of *cd11b*-dnp38 transgene in the murine model

The *cd11b*-dominant negative p38 (*cd11b*-dnp38) mice were backcrossed to C3H/HeN background for > 10 generations. To validate the expression of the transgene (Tg), we performed an RT-PCR with cDNA from lung, thymus and spleen. The expression of the dnp38 transgene was identified in the tissues containing resident macrophages (Fig. 3.6A). We readily detected the expression of the transgene in BMMs (Fig. 3.6A). The *cd11b*-dnp38 Tg mice developed normally and were born at the expected mendelian ratios with no signs of gross abnormalities. The expression of the transgene did not affect macrophage generation or homeostatsis of macrophages, as determined by flow cytometric analysis of splenic F4/80+ in which the percentages of macrophages were similar between the Tg and NLC (Fig. 3.6B).

To confirm that the insertion of the *cd11b*-dnp38 transgene is functional and inhibits the p38 MAP kinase signaling cascade, we analyzed the ability of BMM to produce the proinflammatory cytokines, TNF and IL-6. Following stimulation with live *B. burgdorferi*, Tg macrophages produced significantly less TNF and IL-6 in response to *B. burgdorferi*, than NLC macrophages (Fig. 3.6C), in similar response to RAW264.7 cells treated with the p38 inhibitor SB203580 (47). Overall, these results show that the expression of the transgene does not affect macrophage development and homeostasis but effectively inhibits the activity of the endogenous kinase.

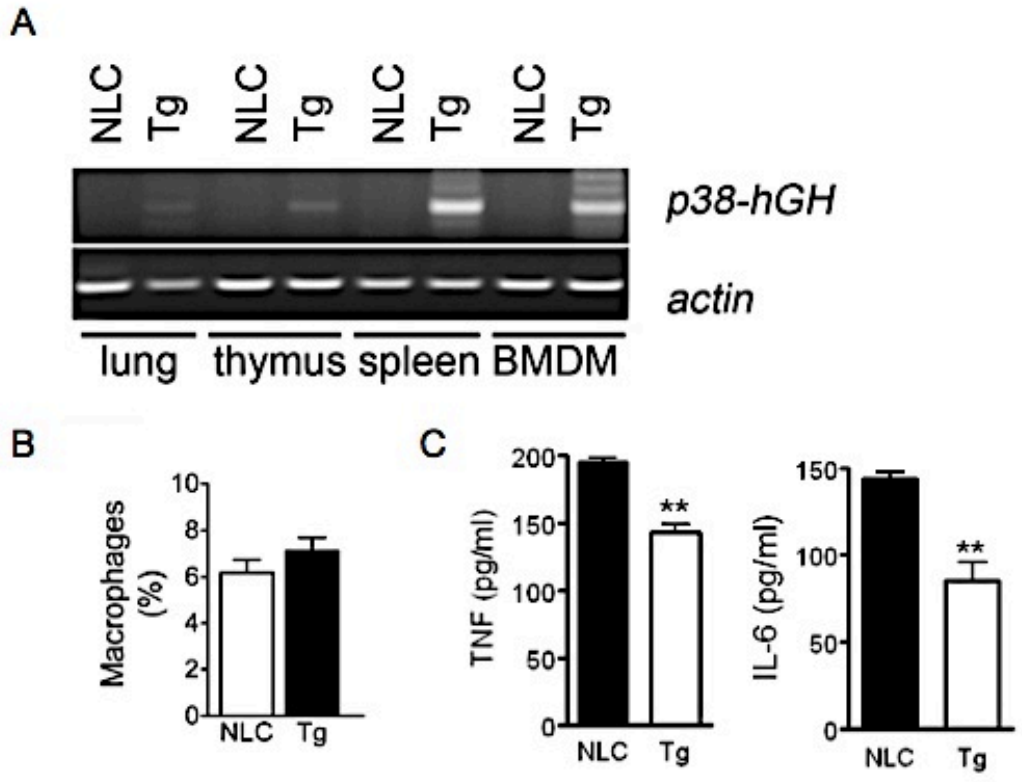

Figure 3.6. Expression of *cd11b*-dnp38 transgene.

(A) Detection of mRNA in different tissues, plus bone marrow derived macrophages (BMDM) by RT-PCR. (B) Percentage of F4/80+ cells in the spleens of Tg and NLC mice. Six to 8 week-old mice were analyzed for macrophage percentage by flow cytometry following staining with an anti-F4/80 mAb. The analysis was performed on gated live cells according to their FSC vs. SSC profile. (C) BMM were incubated with *B. burgdorferi* (m.o.i. = 25) for 6 hours and supernatants were analyzed by ELISA for cytokines levels.

Infection of *cd11b*-dnp38 transgenic mice results in higher bacterial burdens and reduced levels of *ifng* gene expression

We assessed the development of joint and cardiac inflammation in the *cd11b*-dnp38 Tg mice on the C3H/HeN background. The mice were infected and analyzed after 2 weeks of infection. No significant differences were observed in arthritis severity between Tg and NLC mice (Fig. 3.7A). In contrast, the degree of carditis was significantly higher in the Tg animals compared to controls. (Fig. 3.7A & 3.7D)

We determined the bacterial burdens in the skin and heart tissue. Surprisingly, in spite of the identical ability to phagocytose *B. burgdorferi*, the number of spirochetes in the infected hearts of the Tg mice was significantly higher than in infected control mice (Fig. 3.7B & Fig. 3.7C). The antibody response was indistinguishable between the Tg and NLC infected mice (data not shown), indicating that the increased bacterial burden was not due to the generation of a deficient humoral response.

The interplay between cells that infiltrate the heart during infection with *B. burgdorferi* dictates the inflammatory response. The production of IFNγ induces the presentation of spirochetal antigens to iNKT by macrophages, enhances their phagocytic activity and results in the control of inflammation (51). We therefore measured the production of IFNγ in the hearts of the infected mice by qRT-PCR. The level of *ifn*g mRNA in the infected hearts of the Tg mice was significantly reduced compared to NLC animals (Fig. 3.8A), indicating that the inability to control infection locally is the result of the deficient production of the macrophage-activating cytokine.

iNKT cells are major producers of IFNγ during cardiac infection; we therefore measured the infiltration of these cells in the infected tissue. We observed that the number of iNKT cells was significantly reduced in the hearts of the infected Tg mice (Fig. 3.8B). Monocyte chemotactic protein-1 (MCP-1), also known as CCL-2, is a chemokine that has been implicated in the translocation of iNKT cells to the lungs upon infection with *Cryptococcus neomformans*, in addition to tumors of diverse etiology, (115-117). Because of the importance in chemotaxis of iNKT cells, we analyzed the level of expression of the *mcp-1* gene in the hearts of the Tg and NLC mice. The level of *mcp-1* expression was significantly reduced in the *B. burgdorferi* infected hearts of the dnp38 Tg animals compared to the NLC animals (Fig. 3.8C). Moreover, Tg BMM secreted significantly lower basal levels of MCP-1 compared to the NLC in vitro, as well as in response to stimulation with live *B. burgdorferi* (Fig. 3.8D). These results show that p38 MAP kinase regulates the expression of MCP-1, the infiltration of iNKT cells to the heart and production of the protective cytokine, IFNγ in response to *B. burgdorferi*.

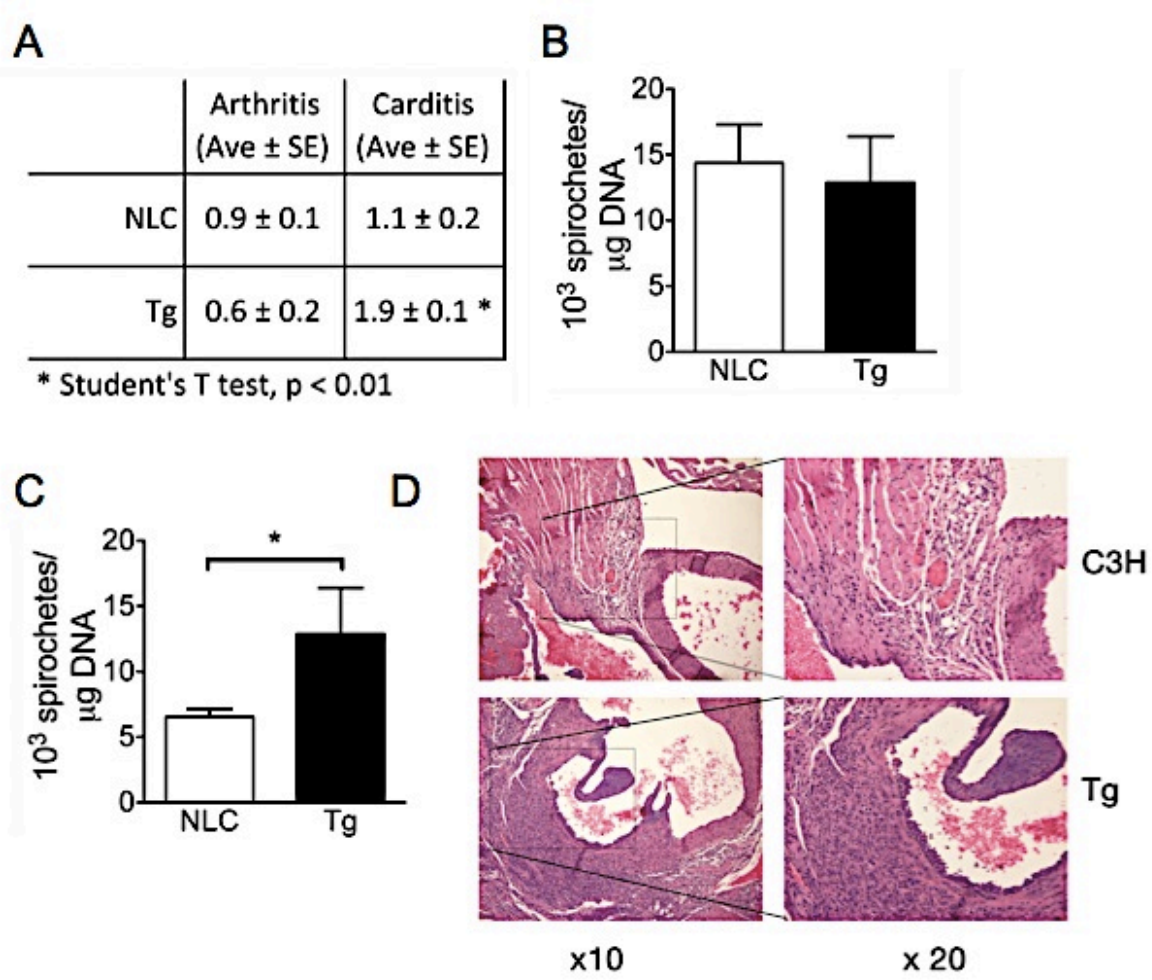

Figure 3.7. Infection of *cd11b*-dnp38 Tg mice with *B. burgdorferi* results in increased carditis.

(A) Arthritis and carditis in 2 week-infected *cd11b*-dnp38 Tg and NLC mice. Groups of mice were infected with *B. burgdorferi* and analyzed for joint and cardiac inflammation. The results represent the average ± SE of 5 mice per group in two independent experiments. *B. burgdorferi* levels in the ear (B) and heart (C) of the Tg and NLC infected mice. (D) Representative hematoxylin and eosin histological sections of the hearts of the infected mice. The results represent the average ± SE of 5 mice per group in two independent experiments.

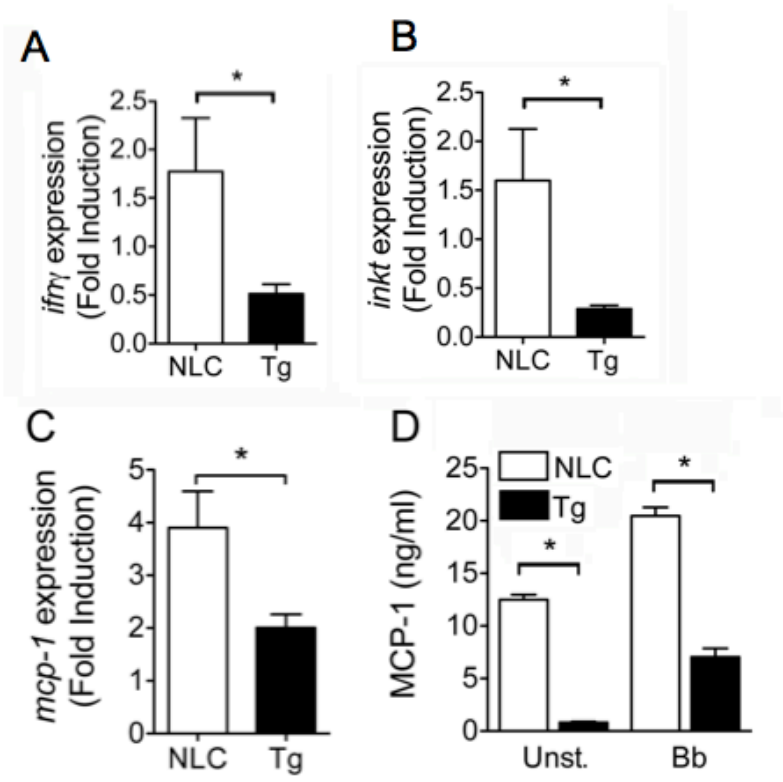

Figure 3.8. Decreased iNKT infiltration and IFNγ production in the hearts of infected Tg mice.

qRT-PCR of Tg (black bars) and NLC (white bars) mouse heart mRNA for the quantification of (A) *ifn*g and (B) *vα14i-jα18* relative to *actin* expression. (C) Relative expression of *mcp-1* in the hearts of Tg and NLC infected mice. mRNA was analyzed by qRT-PCR with primers specific for *mcp-1* and the level of expression was determined relative to *actin*. The results in A-C represent the average ± SE of 10 mice per group from 2 independent experiments. *, Student's *t* test, $p < 0.05$. (D) Production of MCP-1 by Tg and NLC BMMs stimulated with *B. burgdorferi* (m.o.i.= 10) or left unstimulated. The results represent the average ± SE of one experiment performed in triplicate and is representative of three experiments performed. *, Student's *t* test, $p < 0.05$.

CHAPTER IV

CONCLUSIONS

The study of the interaction between macrophages and *B. burgdorferi* has largely focused on the role played by Toll-like receptors and spirochetal lipoproteins. In spite of its importance for controlling bacterial levels at site of inflammation (51) and generating the proinflammatory response of macrophages to the spirochete (33, 76, 85, 93), no receptor associated with phagocytosis of *B. burgdorferi* has been reported. Here, we have identified the β2 integrin, CR3, as a receptor able to mediate the phagocytosis of *B. burgdorferi* both by murine macrophages and human monocytes.

B. burgdorferi has developed mechanisms, known as CRASPs, to protect itself from complement mediated destruction. Two of the CRASP proteins, CspA and OspE-related proteins, are expressed on the surface of the spirochete and bind complement factor H and H-like (98, 100) and down regulate the alternative complement pathway. Our findings demonstrate that serum enhances the internalization of *B. burgdorferi* in a C3-dependent manner and mutations to *B. burgdorferi's* CspA and OspE result in loss of the protective mechanisms resulting in increased bacterial internalization by murine macrophages and human monocytes.

Although CR3 expression alone confers phagocytic capacity to CHO cells for different pathogens and microbial products, including *N. meningitidis* (118), *B. anthracis* spores (62) and zymosan particles (119), this is not the case for *B. burgdoferi*. In several cases, the phagocytic capacity of CR3 is enhanced by, but does not depend on, secondary

receptors. For example, CD14 increases the phagocytic capacity of CR3 through the initiation of inside-out signals that induce the conversion of the integrin from a low to a high affinity conformation. Classically CD14 requires the participation of TLRs, most predominantly TLR2 (62, 71, 72, 120), and involves PI3K activity (62, 72). However, CHO-CR3/CD14 cells do not express a functional TLR2 (112) but nevertheless internalize the spirochete. Consistent with the lack of a functional TLR2, *B. burgdorferi* internalization by CHO-CR3/CD14 cells is independent of MyD88 and PI3K activity. Although activation of CR3 enhances the phagocytic capacity for the spirochetes, integrin activation is not required and MyD88 signals do not contribute to the activation of CR3 in response to *B. burgdorferi*. Even though a significant amount of phagocytosis of *B. burgdorferi* depends on MyD88-derived signals, the internalization of the spirochete still occurs in the absence of the adaptor molecule (33, 110), suggesting that additional pathways are used by macrophages to phagocytose *B. burgdorferi* that are distinctly dependent of MyD88. The identity of the receptor that mediates the MyD88-dependent internalization of the spirochete currently remains unknown. Our observation of phagosomes containing the spirochete in the absence of CR3 strongly supports the theory of the MyD88-dependent receptor. However, our data show that MyD88-independent phagocytosis involves, at least partly, the integrin CR3. Therefore, our results suggest the presence of other receptor(s) on macrophages that contribute to the internalization of the spirochete by macrophages, including those that are MyD88-dependent. The two internalization pathways occurring during the internalization of *B. burgdorferi* are represented in Fig 4.1.

Our results indicate that the role played by CD14 during CR3-mediated phagocytosis of the spirochete involves the localization of the integrin to cholesterol-rich membrane

microdomains, rather than the attachment of *B. burgdorferi*. CD14 would facilitate the clustering of CR3 upon binding to *B. burgdorferi* permitting the initiation of signals that mediate its uptake. In CHO-CR3 cells lacking CD14, the engagement of the C-lectin domain of CR3 is sufficient for the internalization of *B. burgdorferi*. Whether CD14 is unique among GPI-anchored proteins in its ability to promote CR3-dependent phagocytosis of spirochetes remains to be addressed. In the case of *M. kansasii* phagocytosis, for example, several GPI-anchored proteins besides CD14 mediate the uptake of the bacterium, including CD16b, CD66b or CD55 (102). In fact, the lack of a noticeable defect in the phagocytic capacity of CD14-deficient macrophages to take up *B. burgdorferi* (85) suggests the redundant function of other GPI-anchored proteins in CR3-mediated phagocytosis of *B. burgdorferi*.

Cardiac inflammation during infection with *B. burgdorferi* involves the migration and activation of macrophages and other cell types, including invariant NKT and T cells. The production of IFNγ predominantly by iNKT and other cell types ameliorates inflammation through the activation of macrophages (121, 122). The interaction of macrophages and iNKT cells involves feedback mechanisms between both cell types: macrophages present antigen to iNKT cells in the context of the antigen presenting molecule CD1d resulting in IFNγ production; in turn, IFNγ increases both the phagocytic activity of macrophages and the expression of CD1d, thereby increasing their capacity to present antigen to iNKT cells (121). Our results demonstrated that expression of a dominant negative p38 kinase did not alter the macrophages' ability to internalize *B. burgdorferi*; however, infection of *cd11b*-dnp38 transgenic mice reveled increased bacterial burdens and a reduction in *infg* gene expression.

The recruitment of iNKT cells to sites of inflammation or tumors occurs through the expression of chemokines. Several studies have shown that the chemokine MCP-1 (CCL-2) regulates the infiltration of these cells to inflamed tissues and tumors (115, 116, 123), although MCP-1 has been classically associated with the migration of monocytes (124). Our results show that in response to the spirochete, macrophages produce MCP-1 in a p38 MAP kinase-dependent manner. Thus, dnp38 BMMs produce significantly lower levels of the chemokine *in vitro*. Importantly, the expression of *mcp-1* in the Tg infected hearts is significantly reduced compared to controls. Overall, our results support a model in which the colonization of *B. burgdorferi*-infected cardiac tissue by macrophages results in the production of MCP-1. The chemokine induces the infiltration of iNKT cells, whereby macrophages are then able to present galactosyl diacylglycerol antigens from *B. burgdorferi* on the MHC class I-like molecule, CD1d to the iNKT cells (125) resulting in the production of the protective cytokine, IFNγ. Our results show that p38 MAP kinase regulates a critical component in the development of cardiac inflammation.

The infection of CD11b-deficient mice resulted in the development of increased murine Lyme carditis, thus associating the protective capacity of IFNγ (51, 126) controlling the number of spirochetes in the heart of infected mice. Interestingly, stimulating CD11b-deficient macrophages with *B. burgdorferi* significantly increases the production of the proinflammatory cytokine, TNF. Importantly, infecting CD11b-deficient mice also leads to increased expression of the cytokine in the heart. The negative effect of CR3 on macrophage responses to *E. coli* and LPS has been recently reported and involves the degradation of MyD88 and TRIFF by the E3 ubiquitin ligase Cbl-b (108). In light of our results, we propose that the full complement of phagocytic receptors contribute to the internalization of the

bacterium, while at the same time establishing a balance of modulatory (both positive and negative) signals for cytokine production. This suggests that the proinflammatory output of phagocytic cells in response to *B. burgdorferi* is the result of the interplay between the different phagocytic receptors involved in the uptake of the spirochete that eventually determines the strength of the response.

Our results identify CR3 as a receptor able to mediate MyD88-independent phagocytosis of *B. burgdorferi* by murine macrophages and human monocytes. The phagocytic activity of CR3 relies on the cooperation of the GPI-anchored protein CD14 and is independent both of MyD88 and inside-out signals, but does require the translocation of the integrin to cholesterol-rich membrane microdomains. Furthermore, phagocytosis of *B. burgdorferi,* mediated by CR3, results in the modulation of the proinflammatory response of macrophages. Due to the importance of phagocytosis in the overall immune response to the spirochete and the control of infection, these data demonstrate that CR3 is a critical pathogen recognition receptor for *B. burgdorferi*. The identification of CR3 as a *B. burgdorferi* PRR helps clarify the mechanisms that drive not only the physical elimination of the bacteria during infection, but also the integration of the signals emanating from different receptors as a result of phagocytosis.

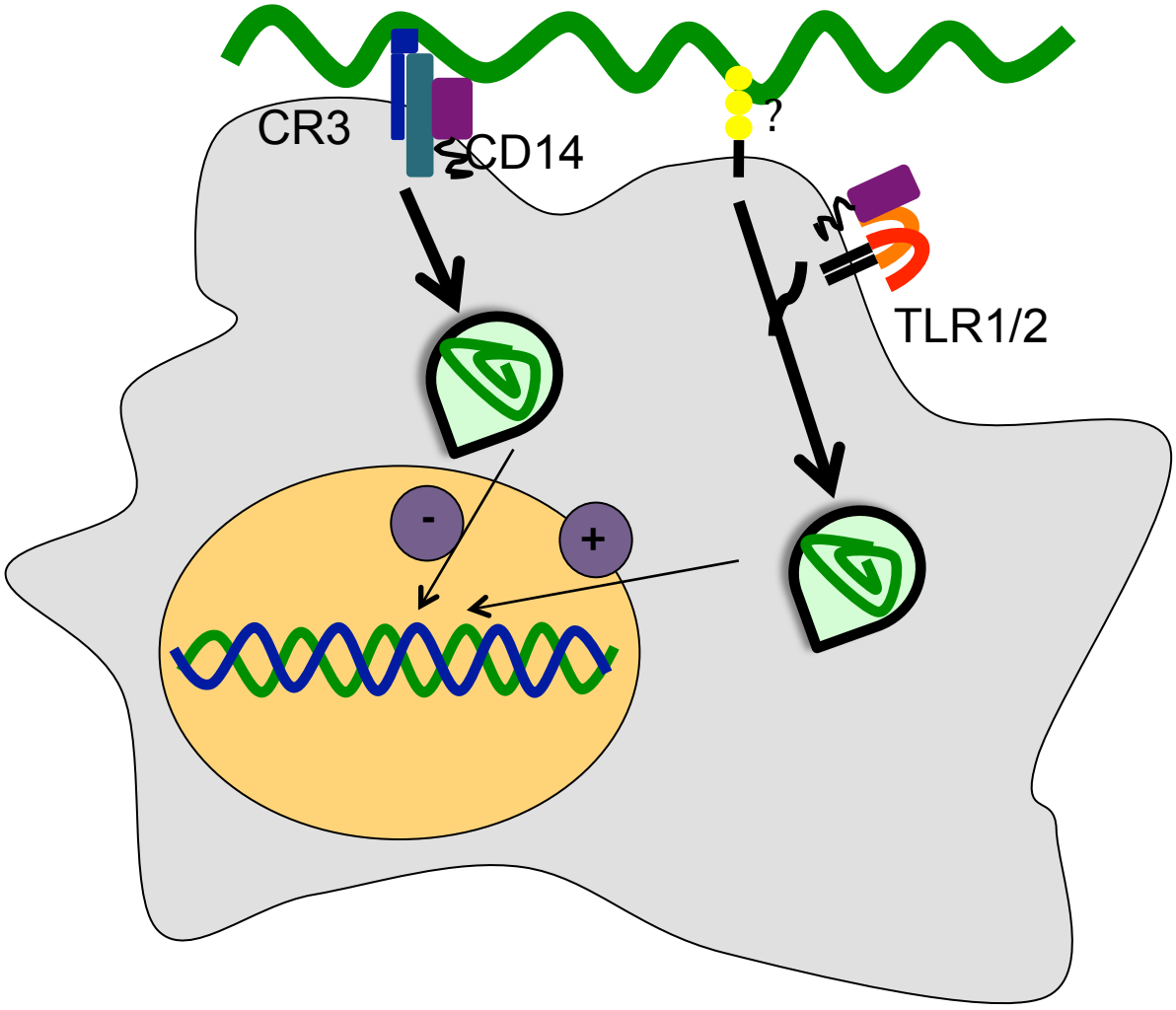

Figure 4.1. Proposed model of internalization signaling.

In response to *B. burgdorferi*, macrophages use at least two signaling pathways. One pathway is CR3-mediated phagocytosis that occurs independent of MyD88 signals and acts as a negative regulation of proinflammatory cytokine production. An additional pathway results in the stimulation of the adaptor molecule, MyD88 and modulation of proinflammatory output of macrophages, mediated by an unidentified receptor.

CHAPTER V

MATERIALS AND METHODS

Mice

C57Bl/6 mice and CD11b-deficient C57Bl/6 mice were purchased from Jackson laboratories and bred at UMass Amherst. For the generation of *cd11b*-dnp38 transgenic mice, the *cd11b*-dnp38 MAP kinase transgene was constructed using the *cd11b* promoter extending from bp -1704 to +83 and included 83 bp of the 5' untranslated region extending up to the ATG codon (a gift from Dr. Daniel G. Tenen), (127). The plasmid also contains a 2.1 kb fragment of the polyadenylation signals and intron sequences of the human growth hormone (128) (Fig. 3.5A). The dnp38 gene was inserted between both sequences by digestion with *Hind* III and *Xba* I. The transgenes were isolated by digestion with *Hind* III and *Not* I and purified by electroelution prior to microinjection into fertilized eggs. The microinjected fertilized eggs were then implanted into pseudopregnant females. Founders were then identified by slot blot using a *Bam* HI-Sac I 0.5 kb fragment from the human growth hormone gene (hGH) and PCR, using the primers (5'-AGG ATC CCA AGG CCC AAC TCC-3' and 5'-CTC CTT AGT CTC CTC CTC TTA T-3'). The transgenic mice have been backcrossed into the C3H/HeN background at least 10 generations to establish stable transgenic mouse lines. The experiments described herein have been obtained using two lines of transgenic mice (171 and 178). The Institutional Animal Care and Use Committee at UMass Amherst approved all procedures involving animals.

Bacteria

The generation and characterization of Bb914, a virulent strain 297 *B. burgdorferi* clone which contains a constitutively expressed *gfp* reporter stably inserted into cp26, as been reported (129). The bacteria were cultured in BSK-II (Sigma) medium at 34ºC and used at mid-log phase of growth.

The CspA mutant and OspE overexpressing spirochetes were a gift from Darrin Akins. In brief, the spirochetes were generated by initially inserting a streptomycin resistance cassette into *cspA* in B31 5A4NP1 then a gentamicin cassette and *flaB-gfp* on cp26 (*cspA* -). The mutation was complemented by inserting a gentamicin *flaB-gfp* and *cpsA* on cp26 (*cspA* +). The *cspA*- stain was electroporated with a shuttle vector that was GFP+ and expressed OspE under the influence of the *flgB* promoter (OspE). As a control, the shuttle vector containing only GFP was electroporated into the *cspA*- (Vector). The bacteria strains were cultured in BSK-II (Sigma) and 40µg/ml gentamicin, 100µg/ml streptomycin and 200µg/ml kanamycin at 34ºC and used at mid-log phase of growth.

Generation of Bone Marrow Macrophages

Bone marrow cells were collected from the femoral shafts and cultured in 20% L929-conditioned RPMI 1640 supplemented with 10% FCS (Hyclone Thermo Scientific, Waltham, MA), 2.4 mM L-glutamine and 10% penicillin- streptomycin (Invitrogen, Carlsbad, CA) in 100 mm x 15 mm petri dishes (Fisher Scientific, Pittsburgh, PA) for 8 days at 37 ºC with 5% CO_2. Following incubation, non-adherent cells were eliminated and adherent macrophages scraped, counted and resuspended in serum-free RPMI medium 2 h prior to use.

Phagocytosis

CHO-cells or macrophages (10^6/ml) were cultured in serum- and antibiotic-free medium with B914 *B. burgdorferi* at different m.o.i. for 4 or 6h, except where indicated. The cells were then washed extensively and resuspended in PBS supplemented with 1% FCS and analyzed by flow cytometry using an LSR II flow cytometer (BD Biosciences) or were further prepared for microscopic analysis. The data were analyzed with FlowJo for Mac, version 7.6 (Tree Star, Inc., Ashland, OR).

In vivo Phagocytosis

Mice were injected intraperitoneally with 10^7 *B. burgdorferi*. The macrophages were harvested after 6 h by peritoneal lavage with 10 mL of ice-cold PBS, stained with mAb F4/80 conjugated with allophycocyanin (APC) (eBioscience) in PBS, 1%FCS for 30 min at 4 °C and analyzed by flow cytometry.

Inhibitor Treatments

RAW264.7 and CHO-CR3/CD14 cells (10^6/ml) were preincubated for 1 hour with 50 μM of a MyD88 inhibitory peptide (InvivoGen, San Diego, CA), 10 μM LY294002 (Cell Signaling Technology, Danvers, MA) or 2 μM wortmannin (Millipore, Temecula, CA), or 30 min with 5 mM of methyl-β-cyclodextran (Sigma Aldrich) at 37°C in serum- and antibiotic-free medium, followed by incubation with *B. burgdorferi* (m.o.i. = 25) for 4 hours.

CD14 Blocking Assay

RAW264.7 and CHO-CR3/CD14 cells (10^6/ml) were preincubated for 1 hour with 10 μg/ml of purified anti-mouse CD14, clone 4C1/CD14 (Biolegend, San Diego CA) or anti-human CD14, clone M5E2 (BD Pharmingen), respectively. For RAW264.7 cells, the isotype control Rat (DA) IgG2b, κ (BD Pharmingen) was used and the isotype control Mouse IgG2a, κ (Biolegend) was used for the CHO-CR3/CD14 cells. Following the phagocytosis assay, spirochetal uptake was measured by flow cytometry, as described above.

Microscopy

To confirm phagocytosis, cells were examined by epifluorescence (ApoTome) and confocal microscopy. Following incubation with bacteria, the cells were washed and fixed in 3.7% paraformaldehyde for 7 minutes. The cells were then permeabilized with 0.1% Triton-X-100 for 5 min and washed. Following blocking of non-specific binding with 5% BSA for 60 minutes, the cells were stained with rhodamine phalloidin to visualize the actin cytoskeleton for 30 minutes at 37 °C and DAPI to stain the nuclei (Invitrogen-Molecular Probes) for 5 minutes at 37 °C. The cells were mounted with Prolong Gold Anti-fade mounting reagent (Invitrogen- Molecular Probes). Photomicrographs were taken using a Zeiss Axiovert 200M inverted microscope (Thornwood, NY) equipped with Apotome and a Hamamatsu Orca camera (Bridgewater, NJ). When noted, the samples were analyzed with a Zeiss LSM 510 Meta Confocal System.

In order to assess the localization of CD11b to lipid rafts, 5 x 10^4 RAW 264.7 cells were incubated with Bb914 (m.o.i 25) for 1 h. The cells were incubated with CTxB the last 20 min of the incubation period, washed and fixed. The preparations were then incubated

with anti-CD11b conjugated to Alexa fluor 647 (M1/70) 2h at RT in the dark. Upon extensive washing, the slides were mounted and analyzed by confocal microscopy.

Cell fractionation by sucrose gradient ultracentrifugation

We performed a detergent extraction method followed by sucrose gradient centrifugation (130), with a few modifications. Briefly, 1 x 10^7 RAW 264.7 cells were stimulated with *B. burgdorferi* (m.o.i. 25) or left unstimulated for 1 h. The cells were washed, resuspended in 200 µl of ice-cold lysis buffer (25 mM MES, pH 6.5, 150 mM NaCl, 1% Triton X-100, 1 mM PMSF, 1 mM NaF, 1 mM Na_3VO_4 and a protein inhibitor cocktail (Sigma-Aldrich)) and disrupted by passage through a 25G syringe. The cell lysate was mixed with an equal volume of 80% sucrose prepared in lysis buffer without TX-100, placed at the bottom of a discontinuous gradient (650 µl of 30% sucrose, 250 µl of 5% sucrose) and centrifuged at 200,000 xg for 20 h at 4 °C. Ten fractions were recovered from the top and precipitated with trichloroacetic acid. The samples were separated in a 10% polyacrylamide gel, transferred to nitrocellulose membranes and immunoblotted with anti-CD11b (M-19) and anti-CD14 (M-305) antibodies (Santa Cruz Biotechnology).

Infection with *B. burgdorferi*

Six to 8 week-old mice were infected by subcutaneous injection with 10^5 *B. burgdorferi* strain 297 in the midline of the back. At 2 to 3 weeks of infection, which represent the acute phase of disease, the mice were sacrificed. Arthritis and carditis were evaluated histologically in formalin-fixed sections processed for H&E staining. The joints were also decalcified. The hearts were cut in half through bisections across the atria and

ventricles prior to sectioning. Signs of arthritis were evaluated based on a combined assessment of histological parameters of *B. burgdorferi*-induced inflammation, such as exudation of fibrin and inflammatory cells into the joints, alteration in the thickness of tendons or ligament sheaths, as well as hypertrophy and hyperplasia of the synovium. Signs of carditis were evaluated based on the cardiac inflammatory infiltrate, including the infiltration of connective tissue with macrophages at the base of the heart, including surrounding the aortic valve and the atria. Carditis was scored on a scale of 0 (no inflammation), 1 (mild inflammation with less than two small foci of infiltration), 2 (moderate inflammation with 2 or more foci of infiltration), or 3 (severe inflammation with focal and diffuse infiltration covering a large area). Both joint and heart tissue sections were blindly examined.

Determination of bacterial burdens

The number of spirochetes in skin (ear) and heart tissue was determined by real-time PCR, using primers specific for the *recA* gene (5'- GTG GAT CTA TTG TAT TAG ATG AGG CTC TCG -3' and 5'- GCC AAA GTT CTG CAA CAT TAA CAC CTA AAG -3') (131) and the fluorescent DNA dye SYBR Green (Roche). Total DNA was extracted by proteinase K-digestion followed by purification using the Qiagen tissue kit following the manufacturer's instructions. PCR conditions were: 40 cycles with denaturing (95 °C) and annealing/extension (60 °C) periods of 30 seconds. Under these conditions, we can detect around 10 spirochetes per pg of total DNA. The number of spirochetes in each sample was standardized to mg of total DNA, as assessed by the use of primers corresponding to *Glyceraldehyde 3-Phosphate Dehydrogenase* (5'-CCA TCA CCA TCT TCC AGG AGC GAG-3' and 5'-CAC AGT CTT CTG GGT GGC AGT GAT-3') by real-time PCR (132).

qRT-PCR

The relative gene expression in cardiac tissue was determined from total RNA extracted from the heart using the TRIzol reagent (Invitrogen, Carlsbad, CA) according to the manufacturer's instructions. The RNA was treated with DNase I (Promega, Madison, WI) and reverse transcribed using oligo dT primers (Invitrogen) and SuperScript II reverse transcriptase (RT) (Invitrogen). The cDNA was amplified in an Mx3005P® QPCR System (Stratagene, La Jolla, CA), using the specific primers listed in Table. 5.1 with SYBR green-containing reaction buffer (Roche, Nutley, NJ). Relative expression of the gene was calculated relative to *actin* levels using the formula $2^{-\Delta Ct}$ and fold induction of the genes were calculated relative to actin values using the $2^{-\Delta\Delta}$Ct method.

Gene	Forward	Reverse
actin	GACGATGCTCCCCGGGCTGTATTC	TCTCTTGCTCTGGGCCTCGTCACC
tnf	AGCCCACGTCGTAGCAAACCA C	ATCGGCTGGCACCACTAGTTGGT
vα14i-jα18	CACCCTGCTGGATGACACTGCC	CTCCAAAATGCAGCCTCCCTAAG
infg	GCGTCATTGAATCACACC	GGACCTGTGGGTTGTTGACC
mcp-1	CGGAACCAAATGAGATCAGAACC	GCTGCAGATTTACGGGTCAACTTC

Table 5.1. qRT-PCR specific primers

Analysis of CR3 affinity conformation

0.5 x 10^6 RAW264.7, CHO-CR3 and CHO-CR3/CD14 cells were preincubated in media for 10 min at 37 °C, followed by incubation with Bb914 (m.o.i. 25) or 1 mM $MnCl_2$ for 30 min. The cells were washed and stained with the mAb CBRM1/5 labeled with Alexa Fluor 647 for 45 min on ice. After incubation, the cells were incubated on ice for 10 min with 1% paraformaldehyde, washed and analyzed by flow cytometry.

Cytokine measurement

The protein levels of MCP-1, IL-6 and TNF in supernatants produced by BMMs were determined by capture ELISA according to manufacturer's recommendations with the BD OptEIA mouse MCP-1, IL-6 and TNF set II ELISA kits (BD Bioscience).

Flow cytometry

10^6 splenocytes were incubated 5 minutes with Fc block (BD pharmigen) followed by 45 minutes at 4 °C with $F4/80_{APC}$ (BM8, eBioscience). The cells were washed and resuspended in PBS 1%FCS for analysis by flow cytometry using an LSR II flow cytometer (BD Biosciences) and analyzed using FlowJo, version 7.6 (Tree Star, Inc.).

To evaluate the surface expression in BMMs, 10^6 cells were incubated 5 minutes with Fc block followed by 45 minutes at 4 °C with $TLR2_{PE}$ (6C2, eBioscience), $CD11b_{PE}$ (M1/70, BD pharmigen) or $CD1d_{PE}$ (1B1, BD pharmigen). The macrophages were washed and analyzed by flow cytometry.

Statistical Analysis

The results are presented as means ± SE. Significant differences between means were calculated with the Student's *t* test. The percentages of infected murine hearts as determined by qPCR were compared by Chi-squared analysis. *p* values of 0.05 or less were considered statistically significant.

BIBLIOGRAPHY

1. Burgdorfer W, Barbour AG, Hayes SF, Benach JL, Grunwaldt E, & Davis JP 1982 Lyme disease-a tick-borne spirochetosis? *Science* 216:1317-1319.

2. Smith RP, Schoen RT, Rahn DW, Sikand VK, Nowakowski J, Parenti DL, Holman MS, Persing DH, & Steere AC 2002 Clinical characteristics and treatment outcome of early Lyme disease in patients with microbiologically confirmed erythema migrans. *Ann Intern Med* 136:421-428.

3. Steere AC 2001 Lyme disease. *N Engl J Med* 345:115-125.

4. Steere AC, Bartenhagen NH, Craft JE, Hutchinson GJ, Newman JH, Rahn DW, Sigal LH, Spieler PN, Stenn KS, & Malawista SE 1983 The early clinical manifestations of Lyme disease. *Ann Intern Med* 99:76-82.

5. LoGiudice K, Ostfeld RS, Schmidt KA, & Keesing F 2003 The ecology of infectious disease: effects of host diversity and community composition on Lyme disease risk. *Proc Natl Acad Sci U S A* 100:567-571.

6. Ge Y, Li C, Corum L, Slaughter CA, & Charon NW 1998 Structure and expression of the FlaA periplasmic flagellar protein of Borrelia burgdorferi. *J Bacteriol* 180:2418-2425.

7. Goldstein SF, Charon NW, & Kreiling JA 1994 Borrelia burgdorferi swims with a planar waveform similar to that of eukaryotic flagella. *Proceedings of the National Academy of Sciences of the United States of America* 91:3433-3437.

8. Fraser CM, Casjens S, Huang WM, Sutton GG, Clayton R, Lathigra R, White O, Ketchum KA, Dodson R, Hickey EK, Gwinn M, Dougherty B, Tomb JF, Fleischmann RD, Richardson D, Peterson J, Kerlavage AR, Quackenbush J, Salzberg S, Hanson M, van Vugt R, Palmer N, Adams MD, Gocayne J, Weidman J, Utterback T, Watthey L, McDonald L, Artiach P, Bowman C, Garland S, Fuji C, Cotton MD, Horst K, Roberts K, Hatch B, Smith HO, & Venter JC 1997 Genomic sequence of a Lyme disease spirochaete, Borrelia burgdorferi. *Nature* 390:580-586.

9. Stevenson B, Schwan TG, & Rosa PA 1995 Temperature-related differential expression of antigens in the Lyme disease spirochete, Borrelia burgdorferi. *Infect Immun* 63:4535-4539.

10. Carroll JA, Cordova RM, & Garon CF 2000 Identification of 11 pH-regulated genes in Borrelia burgdorferi localizing to linear plasmids. *Infect Immun* 68:6677-6684.

11. Pal U, de Silva AM, Montgomery RR, Fish D, Anguita J, Anderson JF, Lobet Y, & Fikrig E 2000 Attachment of Borrelia burgdorferi within Ixodes scapularis mediated by outer surface protein A. *J Clin Invest* 106:561-569.

12. Anguita J, Hedrick MN, & Fikrig E 2003 Adaptation of Borrelia burgdorferi in the tick and the mammalian host. *FEMS Microbiol Rev* 27:493-504.

13. Eggers CH, Caimano MJ, & Radolf JD 2006 Sigma factor selectivity in Borrelia burgdorferi: RpoS recognition of the ospE/ospF/elp promoters is dependent on the sequence of the -10 region. *Mol Microbiol* 59:1859-1875.

14. Tilly K, Krum JG, Bestor A, Jewett MW, Grimm D, Bueschel D, Byram R, Dorward D, Vanraden MJ, Stewart P, & Rosa P 2006 Borrelia burgdorferi OspC protein required exclusively in a crucial early stage of mammalian infection. *Infect Immun* 74:3554-3564.

15. Pal U, Yang X, Chen M, Bockenstedt LK, Anderson JF, Flavell RA, Norgard MV, & Fikrig E 2004 OspC facilitates Borrelia burgdorferi invasion of Ixodes scapularis salivary glands. *J Clin Invest* 113:220-230.

16. Ohnishi J, Piesman J, & de Silva AM 2001 Antigenic and genetic heterogeneity of Borrelia burgdorferi populations transmitted by ticks. *Proc Natl Acad Sci U S A* 98:670-675.

17. Hashimoto C, Hudson KL, & Anderson KV 1988 The Toll gene of Drosophila, required for dorsal-ventral embryonic polarity, appears to encode a transmembrane protein. *Cell* 52:269-279.

18. Lemaitre B, Nicolas E, Michaut L, Reichhart JM, & Hoffmann JA 1996 The dorsoventral regulatory gene cassette spatzle/Toll/cactus controls the potent antifungal response in Drosophila adults. *Cell* 86:973-983.

19. Rock FL, Hardiman G, Timans JC, Kastelein RA, & Bazan JF 1998 A family of human receptors structurally related to Drosophila Toll. *Proc Natl Acad Sci U S A* 95:588-593.

20. Aliprantis AO, Yang RB, Mark MR, Suggett S, Devaux B, Radolf JD, Klimpel GR, Godowski P, & Zychlinsky A 1999 Cell activation and apoptosis by bacterial lipoproteins through toll-like receptor-2. *Science* 285:736-739.

21. Hirschfeld M, Kirschning CJ, Schwandner R, Wesche H, Weis JH, Wooten RM, & Weis JJ 1999 Cutting edge: inflammatory signaling by Borrelia burgdorferi lipoproteins is mediated by toll-like receptor 2. *Journal of immunology* 163:2382-2386.

22. Alexopoulou L, Thomas V, Schnare M, Lobet Y, Anguita J, Schoen RT, Medzhitov R, Fikrig E, & Flavell RA 2002 Hyporesponsiveness to vaccination with Borrelia burgdorferi OspA in humans and in TLR1- and TLR2-deficient mice. *Nat Med* 8:878-884.

23. Sellati TJ, Bouis DA, Caimano MJ, Feulner JA, Ayers C, Lien E, & Radolf JD 1999 Activation of human monocytic cells by Borrelia burgdorferi and Treponema pallidum is facilitated by CD14 and correlates with surface exposure of spirochetal lipoproteins. *Journal of immunology* 163:2049-2056.

24. Radolf JD, Norgard MV, Brandt ME, Isaacs RD, Thompson PA, & Beutler B 1991 Lipoproteins of Borrelia burgdorferi and Treponema pallidum activate cachectin/tumor necrosis factor synthesis. Analysis using a CAT reporter construct. *Journal of immunology* 147:1968-1974.

25. Radolf JD, Arndt LL, Akins DR, Curetty LL, Levi ME, Shen Y, Davis LS, & Norgard MV 1995 Treponema pallidum and Borrelia burgdorferi lipoproteins and synthetic lipopeptides activate monocytes/macrophages. *Journal of immunology* 154:2866-2877.

26. Cervantes JL, Dunham-Ems SM, La Vake CJ, Petzke MM, Sahay B, Sellati TJ, Radolf JD, & Salazar JC 2011 Phagosomal signaling by Borrelia burgdorferi in human monocytes involves Toll-like receptor (TLR) 2 and TLR8 cooperativity and TLR8-mediated induction of IFN-beta. *Proc Natl Acad Sci U S A* 108:3683-3688.

27. Akira S, Uematsu S, & Takeuchi O 2006 Pathogen recognition and innate immunity. *Cell* 124:783-801.

28. Kumar H, Kawai T, & Akira S 2009 Toll-like receptors and innate immunity. *Biochem Biophys Res Commun* 388:621-625.

29. Guerau-de-Arellano M & Huber BT 2005 Chemokines and Toll-like receptors in Lyme disease pathogenesis. *Trends Mol Med* 11:114-120.

30. Bolz DD, Sundsbak RS, Ma Y, Akira S, Kirschning CJ, Zachary JF, Weis JH, & Weis JJ 2004 MyD88 plays a unique role in host defense but not arthritis development in Lyme disease. *J Immunol* 173:2003-2010.

31. Liu N, Montgomery RR, Barthold SW, & Bockenstedt LK 2004 Myeloid differentiation antigen 88 deficiency impairs pathogen clearance but does not alter inflammation in Borrelia burgdorferi-infected mice. *Infect Immun* 72:3195-3203.

32. Salazar JC, Duhnam-Ems S, La Vake C, Cruz AR, Moore MW, Caimano MJ, Velez-Climent L, Shupe J, Krueger W, & Radolf JD 2009 Activation of human monocytes by live Borrelia burgdorferi generates TLR2-dependent and -independent responses which include induction of IFN-beta. *PLoS Pathog* 5:e1000444.

33. Shin OS, Isberg RR, Akira S, Uematsu S, Behera AK, & Hu LT 2008 Distinct roles for MyD88 and Toll-like receptors 2, 5, and 9 in phagocytosis of Borrelia burgdorferi and cytokine induction. *Infect Immun* 76:2341-2351.

34. Raingeaud J, Gupta S, Rogers JS, Dickens M, Han J, Ulevitch RJ, & Davis RJ 1995 Pro-inflammatory cytokines and environmental stress cause p38 mitogen-activated protein kinase activation by dual phosphorylation on tyrosine and threonine. *The Journal of biological chemistry* 270:7420-7426.

35. Freshney NW, Rawlinson L, Guesdon F, Jones E, Cowley S, Hsuan J, & Saklatvala J 1994 Interleukin-1 activates a novel protein kinase cascade that results in the phosphorylation of Hsp27. *Cell* 78:1039-1049.

36. Olson CM, Hedrick MN, Izadi H, Bates TC, Olivera ER, & Anguita J 2007 p38 mitogen-activated protein kinase controls NF-kappaB transcriptional activation and tumor necrosis factor alpha production through RelA phosphorylation mediated by mitogen- and stress-activated protein kinase 1 in response to Borrelia burgdorferi antigens. *Infection and immunity* 75:270-277.

37. Han J, Lee JD, Bibbs L, & Ulevitch RJ 1994 A MAP kinase targeted by endotoxin and hyperosmolarity in mammalian cells. *Science* 265:808-811.

38. Miller CL, Lee JH, Kieff E, Burkhardt AL, Bolen JB, & Longnecker R 1994 Epstein-Barr virus protein LMP2A regulates reactivation from latency by negatively regulating tyrosine kinases involved in sIg-mediated signal transduction. *Infect Agents Dis* 3:128-136.

39. Rouse J, Cohen P, Trigon S, Morange M, Alonso-Llamazares A, Zamanillo D, Hunt T, & Nebreda AR 1994 A novel kinase cascade triggered by stress and heat shock that stimulates MAPKAP kinase-2 and phosphorylation of the small heat shock proteins. *Cell* 78:1027-1037.

40. Ip YT & Davis RJ 1998 Signal transduction by the c-Jun N-terminal kinase (JNK)--from inflammation to development. *Curr Opin Cell Biol* 10:205-219.

41. Whitmarsh AJ & Davis RJ 1996 Transcription factor AP-1 regulation by mitogen-activated protein kinase signal transduction pathways. *J Mol Med (Berl)* 74:589-607.

42. Derijard B, Hibi M, Wu IH, Barrett T, Su B, Deng T, Karin M, & Davis RJ 1994 JNK1: a protein kinase stimulated by UV light and Ha-Ras that binds and phosphorylates the c-Jun activation domain. *Cell* 76:1025-1037.

43. Derijard B, Raingeaud J, Barrett T, Wu IH, Han J, Ulevitch RJ, & Davis RJ 1995 Independent human MAP-kinase signal transduction pathways defined by MEK and MKK isoforms. *Science* 267:682-685.

44. Han J, Lee JD, Jiang Y, Li Z, Feng L, & Ulevitch RJ 1996 Characterization of the structure and function of a novel MAP kinase kinase (MKK6). *The Journal of biological chemistry* 271:2886-2891.

45. Moriguchi T, Kuroyanagi N, Yamaguchi K, Gotoh Y, Irie K, Kano T, Shirakabe K, Muro Y, Shibuya H, Matsumoto K, Nishida E, & Hagiwara M 1996 A novel kinase cascade mediated by mitogen-activated protein kinase kinase 6 and MKK3. *The Journal of biological chemistry* 271:13675-13679.

46. Raingeaud J, Whitmarsh AJ, Barrett T, Derijard B, & Davis RJ 1996 MKK3- and MKK6-regulated gene expression is mediated by the p38 mitogen-activated protein kinase signal transduction pathway. *Mol Cell Biol* 16:1247-1255.

47. Anguita J, Barthold SW, Persinski R, Hedrick MN, Huy CA, Davis RJ, Flavell RA, & Fikrig E 2002 Murine Lyme arthritis development mediated by p38 mitogen-activated protein kinase activity. *Journal of immunology* 168:6352-6357.

48. Cinco M, Cini B, Murgia R, Presani G, Prodan M, & Perticarari S 2001 Evidence of involvement of the mannose receptor in adhesion of Borrelia burgdorferi to monocyte/macrophages. *Infect Immun* 69:2743-2747.

49. Coburn J & Cugini C 2003 Targeted mutation of the outer membrane protein P66 disrupts attachment of the Lyme disease agent, Borrelia burgdorferi, to integrin alphavbeta3. *Proc Natl Acad Sci U S A* 100:7301-7306.

50. Behera AK, Hildebrand E, Uematsu S, Akira S, Coburn J, & Hu LT 2006 Identification of a TLR-independent pathway for Borrelia burgdorferi-induced expression of matrix metalloproteinases and inflammatory mediators through binding to integrin alpha 3 beta 1. *J Immunol* 177:657-664.

51. Olson CM, Jr., Bates TC, Izadi H, Radolf JD, Huber SA, Boyson JE, & Anguita J 2009 Local production of IFN-gamma by invariant NKT cells modulates acute Lyme carditis. *J Immunol* 182:3728-3734.

52. Moore MW, Cruz AR, LaVake CJ, Marzo AL, Eggers CH, Salazar JC, & Radolf JD 2007 Phagocytosis of Borrelia burgdorferi and Treponema pallidum potentiates innate immune activation and induces gamma interferon production. *Infect Immun* 75:2046-2062.

53. Lawrenz MB, Wooten RM, Zachary JF, Drouin SM, Weis JJ, Wetsel RA, & Norris SJ 2003 Effect of complement component C3 deficiency on experimental Lyme borreliosis in mice. *Infection and immunity* 71:4432-4440.

54. Kochi SK & Johnson RC 1988 Role of immunoglobulin G in killing of Borrelia burgdorferi by the classical complement pathway. *Infection and immunity* 56:314-321.

55. Hellwage J, Meri T, Heikkila T, Alitalo A, Panelius J, Lahdenne P, Seppala IJ, & Meri S 2001 The complement regulator factor H binds to the surface protein OspE of Borrelia burgdorferi. *The Journal of biological chemistry* 276:8427-8435.

56. Kraiczy P, Hellwage J, Skerka C, Becker H, Kirschfink M, Simon MM, Brade V, Zipfel PF, & Wallich R 2004 Complement resistance of Borrelia burgdorferi correlates with the expression of BbCRASP-1, a novel linear plasmid-encoded surface protein that interacts with human factor H and FHL-1 and is unrelated to Erp proteins. *The Journal of biological chemistry* 279:2421-2429.

57. Kraiczy P, Skerka C, Kirschfink M, Brade V, & Zipfel PF 2001 Immune evasion of Borrelia burgdorferi by acquisition of human complement regulators FHL-1/reconectin and Factor H. *European journal of immunology* 31:1674-1684.

58. Humphries MJ 2000 Integrin structure. *Biochem Soc Trans* 28:311-339.

59. Ehlers MR 2000 CR3: a general purpose adhesion-recognition receptor essential for innate immunity. *Microbes Infect* 2:289-294.

60. Hovius JW, Bijlsma MF, van der Windt GJ, Wiersinga WJ, Boukens BJ, Coumou J, Oei A, de Beer R, de Vos AF, van 't Veer C, van Dam AP, Wang P, Fikrig E, Levi MM, Roelofs JJ, & van der Poll T 2009 The urokinase receptor (uPAR) facilitates clearance of Borrelia burgdorferi. *PLoS Pathog* 5:e1000447.

61. Pliyev BK, Arefieva TI, & Menshikov MY 2010 Urokinase receptor (uPAR) regulates complement receptor 3 (CR3)-mediated neutrophil phagocytosis. *Biochem Biophys Res Commun* 397:277-282.

62. Oliva C, Turnbough CL, Jr., & Kearney JF 2009 CD14-Mac-1 interactions in Bacillus anthracis spore internalization by macrophages. *Proc Natl Acad Sci U S A* 106:13957-13962.

63. Cinco M, Murgia R, Presani G, & Perticarari S 1997 Integrin CR3 mediates the binding of nonspecifically opsonized Borrelia burgdorferi to human phagocytes and mammalian cells. *Infect Immun* 65:4784-4789.

64. Cinco M, Murgia R, Perticarari S, & Presani G 1998 Surface receptors of neutrophils towards B. burgdorferi. *Wien Klin Wochenschr* 110:866-869.

65. Garcia RC, Murgia R, & Cinco M 2005 Complement receptor 3 binds the Borrelia burgdorferi outer surface proteins OspA and OspB in an iC3b-independent manner. *Infection and immunity* 73:6138-6142.

66. Hynes RO 1992 Integrins: versatility, modulation, and signaling in cell adhesion. *Cell* 69:11-25.

67. Qin J, Vinogradova O, & Plow EF 2004 Integrin bidirectional signaling: a molecular view. *PLoS Biol* 2:e169.

68. Hynes RO & Lander AD 1992 Contact and adhesive specificities in the associations, migrations, and targeting of cells and axons. *Cell* 68:303-322.

69. Hynes RO 2002 Integrins: bidirectional, allosteric signaling machines. *Cell* 110:673-687.

70. Liddington RC & Ginsberg MH 2002 Integrin activation takes shape. *J Cell Biol* 158:833-839.

71. Sendide K, Reiner NE, Lee JS, Bourgoin S, Talal A, & Hmama Z 2005 Cross-talk between CD14 and complement receptor 3 promotes phagocytosis of mycobacteria: regulation by phosphatidylinositol 3-kinase and cytohesin-1. *J Immunol* 174:4210-4219.

72. Harokopakis E & Hajishengallis G 2005 Integrin activation by bacterial fimbriae through a pathway involving CD14, Toll-like receptor 2, and phosphatidylinositol-3-kinase. *Eur J Immunol* 35:1201-1210.

73. Vachon E, Martin R, Kwok V, Cherepanov V, Chow CW, Doerschuk CM, Plumb J, Grinstein S, & Downey GP 2007 CD44-mediated phagocytosis induces inside-out activation of complement receptor-3 in murine macrophages. *Blood* 110:4492-4502.

74. van Spriel AB, van Ojik HH, Bakker A, Jansen MJ, & van de Winkel JG 2003 Mac-1 (CD11b/CD18) is crucial for effective Fc receptor-mediated immunity to melanoma. *Blood* 101:253-258.

75. Means TK & Luster AD 2010 Integrins limit the Toll. *Nature immunology* 11:691-693.

76. Moore KJ, Andersson LP, Ingalls RR, Monks BG, Li R, Arnaout MA, Golenbock DT, & Freeman MW 2000 Divergent response to LPS and bacteria in CD14-deficient murine macrophages. *Journal of immunology* 165:4272-4280.

77. Fitzgerald KA, Rowe DC, & Golenbock DT 2004 Endotoxin recognition and signal transduction by the TLR4/MD2-complex. *Microbes and infection / Institut Pasteur* 6:1361-1367.

78. Baumann CL, Aspalter IM, Sharif O, Pichlmair A, Bluml S, Grebien F, Bruckner M, Pasierbek P, Aumayr K, Planyavsky M, Bennett KL, Colinge J, Knapp S, & Superti-Furga G 2010 CD14 is a coreceptor of Toll-like receptors 7 and 9. *J Exp Med* 207:2689-2701.

79. Pugin J, Heumann ID, Tomasz A, Kravchenko VV, Akamatsu Y, Nishijima M, Glauser MP, Tobias PS, & Ulevitch RJ 1994 CD14 is a pattern recognition receptor. *Immunity* 1:509-516.

80. Kusunoki T, Hailman E, Juan TS, Lichenstein HS, & Wright SD 1995 Molecules from Staphylococcus aureus that bind CD14 and stimulate innate immune responses. *J Exp Med* 182:1673-1682.

81. Zhang Y, Doerfler M, Lee TC, Guillemin B, & Rom WN 1993 Mechanisms of stimulation of interleukin-1 beta and tumor necrosis factor-alpha by Mycobacterium tuberculosis components. *The Journal of clinical investigation* 91:2076-2083.

82. Wooten RM, Morrison TB, Weis JH, Wright SD, Thieringer R, & Weis JJ 1998 The role of CD14 in signaling mediated by outer membrane lipoproteins of Borrelia burgdorferi. *Journal of immunology* 160:5485-5492.

83. Zanoni I, Ostuni R, Marek LR, Barresi S, Barbalat R, Barton GM, Granucci F, & Kagan JC 2011 CD14 controls the LPS-induced endocytosis of Toll-like receptor 4. *Cell* 147:868-880.

84. Sellati TJ, Bouis DA, Kitchens RL, Darveau RP, Pugin J, Ulevitch RJ, Gangloff SC, Goyert SM, Norgard MV, & Radolf JD 1998 Treponema pallidum and Borrelia burgdorferi lipoproteins and synthetic lipopeptides activate monocytic cells via a CD14-dependent pathway distinct from that used by lipopolysaccharide. *Journal of immunology* 160:5455-5464.

85. Sahay B, Patsey RL, Eggers CH, Salazar JC, Radolf JD, & Sellati TJ 2009 CD14 signaling restrains chronic inflammation through induction of p38-MAPK/SOCS-dependent tolerance. *PLoS Pathog* 5:e1000687.

86. Bohuslav J, Horejsi V, Hansmann C, Stockl J, Weidle UH, Majdic O, Bartke I, Knapp W, & Stockinger H 1995 Urokinase plasminogen activator receptor, beta 2-integrins, and Src-kinases within a single receptor complex of human monocytes. *J Exp Med* 181:1381-1390.

87. Sitrin RG, Todd RF, 3rd, Albrecht E, & Gyetko MR 1996 The urokinase receptor (CD87) facilitates CD11b/CD18-mediated adhesion of human monocytes. *The Journal of clinical investigation* 97:1942-1951.

88. Vance RE, Isberg RR, & Portnoy DA 2009 Patterns of pathogenesis: discrimination of pathogenic and nonpathogenic microbes by the innate immune system. *Cell Host Microbe* 6:10-21.

89. von Koenig CH, Finger H, & Hof H 1982 Failure of killed Listeria monocytogenes vaccine to produce protective immunity. *Nature* 297:233-234.

90. Lauvau G, Vijh S, Kong P, Horng T, Kerksiek K, Serbina N, Tuma RA, & Pamer EG 2001 Priming of memory but not effector CD8 T cells by a killed bacterial vaccine. *Science* 294:1735-1739.

91. Kasturi SP, Skountzou I, Albrecht RA, Koutsonanos D, Hua T, Nakaya HI, Ravindran R, Stewart S, Alam M, Kwissa M, Villinger F, Murthy N, Steel J, Jacob J, Hogan RJ, Garcia-Sastre A, Compans R, & Pulendran B 2011 Programming the magnitude and persistence of antibody responses with innate immunity. *Nature* 470:543-547.

92. Sander LE, Davis MJ, Boekschoten MV, Amsen D, Dascher CC, Ryffel B, Swanson JA, Muller M, & Blander JM 2011 Detection of prokaryotic mRNA signifies microbial viability and promotes immunity. *Nature* 474:385-389.

93. Petzke MM, Brooks A, Krupna MA, Mordue D, & Schwartz I 2009 Recognition of Borrelia burgdorferi, the Lyme disease spirochete, by TLR7 and TLR9 induces a type I IFN response by human immune cells. *Journal of immunology* 183:5279-5292.

94. Radolf JD, Caimano MJ, Stevenson B, & Hu LT 2012 Of ticks, mice and men: understanding the dual-host lifestyle of Lyme disease spirochaetes. *Nat Rev Microbiol* 10:87-99.

95. Amiel E, Acker JL, Collins RM, & Berwin B 2009 Uncoupling scavenger receptor A-mediated phagocytosis of bacteria from endotoxic shock resistance. *Infection and immunity* 77:4567-4573.

96. Hartmann K, Corvey C, Skerka C, Kirschfink M, Karas M, Brade V, Miller JC, Stevenson B, Wallich R, Zipfel PF, & Kraiczy P 2006 Functional characterization of BbCRASP-2, a distinct outer membrane protein of Borrelia burgdorferi that binds host complement regulators factor H and FHL-1. *Molecular microbiology* 61:1220-1236.

97. Brooks CS, Vuppala SR, Jett AM, Alitalo A, Meri S, & Akins DR 2005 Complement regulator-acquiring surface protein 1 imparts resistance to human serum in Borrelia burgdorferi. *Journal of immunology* 175:3299-3308.

98. Kenedy MR, Vuppala SR, Siegel C, Kraiczy P, & Akins DR 2009 CspA-mediated binding of human factor H inhibits complement deposition and confers serum resistance in Borrelia burgdorferi. *Infection and immunity* 77:2773-2782.

99. Coleman AS, Yang X, Kumar M, Zhang X, Promnares K, Shroder D, Kenedy MR, Anderson JF, Akins DR, & Pal U 2008 Borrelia burgdorferi complement regulator-acquiring surface protein 2 does not contribute to complement resistance or host infectivity. *PLoS One* 3:3010e.

100. Kenedy MR & Akins DR 2011 The OspE-related proteins inhibit complement deposition and enhance serum resistance of Borrelia burgdorferi, the lyme disease spirochete. *Infection and immunity* 79:1451-1457.

101. Ross GD 2002 Role of the lectin domain of Mac-1/CR3 (CD11b/CD18) in regulating intercellular adhesion. *Immunol Res* 25:219-227.

102. Peyron P, Bordier C, N'Diaye EN, & Maridonneau-Parini I 2000 Nonopsonic phagocytosis of Mycobacterium kansasii by human neutrophils depends on cholesterol and is mediated by CR3 associated with glycosylphosphatidylinositol-anchored proteins. *J Immunol* 165:5186-5191.

103. Golenbock DT, Liu Y, Millham FH, Freeman MW, & Zoeller RA 1993 Surface expression of human CD14 in Chinese hamster ovary fibroblasts imparts macrophage-like responsiveness to bacterial endotoxin. *J Biol Chem* 268:22055-22059.

104. Power CP, Wang JH, Manning B, Kell MR, Aherne NJ, Wu QD, & Redmond HP 2004 Bacterial lipoprotein delays apoptosis in human neutrophils through inhibition of caspase-3 activity: regulatory roles for CD14 and TLR-2. *Journal of immunology* 173:5229-5237.

105. Triantafilou M, Morath S, Mackie A, Hartung T, & Triantafilou K 2004 Lateral diffusion of Toll-like receptors reveals that they are transiently confined within lipid rafts on the plasma membrane. *J Cell Sci* 117:4007-4014.

106. Aman AT, Fraser S, Merritt EA, Rodigherio C, Kenny M, Ahn M, Hol WG, Williams NA, Lencer WI, & Hirst TR 2001 A mutant cholera toxin B subunit that binds GM1-ganglioside but lacks immunomodulatory or toxic activity. *Proceedings of the National Academy of Sciences of the United States of America* 98:8536-8541.

107. Lafont F, Tran Van Nhieu G, Hanada K, Sansonetti P, & van der Goot FG 2002 Initial steps of Shigella infection depend on the cholesterol/sphingolipid raft-mediated CD44-IpaB interaction. *Embo J* 21:4449-4457.

108. Han C, Jin J, Xu S, Liu H, Li N, & Cao X 2010 Integrin CD11b negatively regulates TLR-triggered inflammatory responses by activating Syk and promoting degradation of MyD88 and TRIF via Cbl-b. *Nat Immunol* 11:734-742.

109. Benhnia MR, Wroblewski D, Akhtar MN, Patel RA, Lavezzi W, Gangloff SC, Goyert SM, Caimano MJ, Radolf JD, & Sellati TJ 2005 Signaling through CD14 attenuates the inflammatory response to Borrelia burgdorferi, the agent of Lyme disease. *J Immunol* 174:1539-1548.

110. Shin OS, Miller LS, Modlin RL, Akira S, Uematsu S, & Hu LT 2009 Downstream signals for MyD88-mediated phagocytosis of Borrelia burgdorferi can be initiated by TRIF and are dependent on PI3K. *Journal of immunology* 183:491-498.

111. Ross GD 2000 Regulation of the adhesion versus cytotoxic functions of the Mac-1/CR3/alphaMbeta2-integrin glycoprotein. *Crit Rev Immunol* 20:197-222.

112. Heine H, Kirschning CJ, Lien E, Monks BG, Rothe M, & Golenbock DT 1999 Cutting edge: cells that carry A null allele for toll-like receptor 2 are capable of responding to endotoxin. *J Immunol* 162:6971-6975.

113. Blander JM & Medzhitov R 2004 Regulation of phagosome maturation by signals from toll-like receptors. *Science* 304:1014-1018.

114. Rincon M, Enslen H, Raingeaud J, Recht M, Zapton T, Su MS, Penix LA, Davis RJ, & Flavell RA 1998 Interferon-gamma expression by Th1 effector T cells mediated by the p38 MAP kinase signaling pathway. *Embo J* 17:2817-2829.

115. Nowak M, Arredouani MS, Tun-Kyi A, Schmidt-Wolf I, Sanda MG, Balk SP, & Exley MA 2010 Defective NKT cell activation by CD1d+ TRAMP prostate tumor cells is corrected by interleukin-12 with alpha-galactosylceramide. *PLoS One* 5:e11311.

116. Song L, Ara T, Wu HW, Woo CW, Reynolds CP, Seeger RC, DeClerck YA, Thiele CJ, Sposto R, & Metelitsa LS 2007 Oncogene MYCN regulates localization of NKT cells to the site of disease in neuroblastoma. *The Journal of clinical investigation* 117:2702-2712.

117. Kawakami K, Kinjo Y, Uezu K, Yara S, Miyagi K, Koguchi Y, Nakayama T, Taniguchi M, & Saito A 2001 Monocyte chemoattractant protein-1-dependent increase of V alpha 14 NKT cells in lungs and their roles in Th1 response and host defense in cryptococcal infection. *Journal of immunology* 167:6525-6532.

118. Jones HE, Strid J, Osman M, Uronen-Hansson H, Dixon G, Klein N, Wong SY, & Callard RE 2008 The role of beta2 integrins and lipopolysaccharide-binding protein in the phagocytosis of dead Neisseria meningitidis. *Cell Microbiol* 10:1634-1645.

119. Le Cabec V, Cols C, & Maridonneau-Parini I 2000 Nonopsonic phagocytosis of zymosan and Mycobacterium kansasii by CR3 (CD11b/CD18) involves distinct molecular determinants and is or is not coupled with NADPH oxidase activation. *Infection and immunity* 68:4736-4745.

120. Hajishengallis G, Wang M, Liang S, Shakhatreh MA, James D, Nishiyama S, Yoshimura F, & Demuth DR 2008 Subversion of innate immunity by periodontopathic bacteria via exploitation of complement receptor-3. *Adv Exp Med Biol* 632:203-219.

121. Olson CM, Jr., Bates TC, Izadi H, Radolf JD, Huber SA, Boyson JE, & Anguita J 2009 Local Production of IFN-{gamma} by Invariant NKT Cells Modulates Acute Lyme Carditis. *J Immunol* 182:3728-3734.

122. Bockenstedt LK, Kang I, Chang C, Persing D, Hayday A, & Barthold SW 2001 $CD4^+$ T helper 1 cells facilitate regression of murine Lyme carditis. *Infect Immun* 69:5264-5269.

123. Kawakami K, Kinjo Y, Uezu K, Yara S, Miyagi K, Koguchi Y, Nakayama T, Taniguchi M, & Saito A 2001 Monocyte chemoattractant protein-1-dependent increase of V alpha 14 NKT cells in lungs and their roles in Th1 response and host defense in cryptococcal infection. *J Immunol* 167:6525-6532.

124. Yadav A, Saini V, & Arora S 2010 MCP-1: chemoattractant with a role beyond immunity: a review. *Clinica chimica acta; international journal of clinical chemistry* 411:1570-1579.

125. Kinjo Y, Tupin E, Wu D, Fujio M, Garcia-Navarro R, Benhnia MR, Zajonc DM, Ben-Menachem G, Ainge GD, Painter GF, Khurana A, Hoebe K, Behar SM, Beutler B, Wilson IA, Tsuji M, Sellati TJ, Wong CH, & Kronenberg M 2006 Natural killer T cells recognize diacylglycerol antigens from pathogenic bacteria. *Nature immunology* 7:978-986.

126. Bockenstedt LK, Kang I, Chang C, Persing D, Hayday A, & Barthold SW 2001 CD4+ T helper 1 cells facilitate regression of murine Lyme carditis. *Infection and immunity* 69:5264-5269.

127. Dziennis S, Van Etten RA, Pahl HL, Morris DL, Rothstein TL, Blosch CM, Perlmutter RM, & Tenen DG 1995 The CD11b promoter directs high-level expression of reporter genes in macrophages in transgenic mice. *Blood* 85:319-329.

128. Rincón M, Enslen H, Raingeaud J, Recht M, Zapton T, Su MS, Penix LA, Davis RJ, & Flavell RA 1998 Interferon-gamma expression by Th1 effector T cells mediated by the p38 MAP kinase signaling pathway. *EMBO J* 17:2817-2829.

129. Dunham-Ems SM, Caimano MJ, Pal U, Wolgemuth CW, Eggers CH, Balic A, & Radolf JD 2009 Live imaging reveals a biphasic mode of dissemination of Borrelia burgdorferi within ticks. *J Clin Invest* 119:3652-3665.

130. Zhu X, Owen JS, Wilson MD, Li H, Griffiths GL, Thomas MJ, Hiltbold EM, Fessler MB, & Parks JS 2010 Macrophage ABCA1 reduces MyD88-dependent Toll-like receptor trafficking to lipid rafts by reduction of lipid raft cholesterol. *J Lipid Res* 51:3196-3206.

131. Morrison TB, Ma Y, Weis JH, & Weis JJ 1999 Rapid and sensitive quantification of *Borrelia burgdorferi*-infected mouse tissues by continuous fluorescent monitoring of PCR. *J Clin Microbiol* 37:987-992.

132. Motameni AR, Bates TC, Juncadella IJ, Petty C, Hedrick MN, & Anguita J 2005 Distinct bacterial dissemination and disease outcome in mice subcutaneously infected with Borrelia burgdorferi in the midline of the back and the footpad. *FEMS immunology and medical microbiology* 45:279-284.